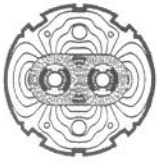

LHC Project Note 106

1997-09-15

(laurent.tavian@cern.ch)

A proposal for simplication of the LHC cryogenic scheme

M. Chorowski, B. Hilbert, Ph. Lebrun, L. Serio, L. Tavian, U. Wagner, R. van Weelderen
LHC-ACR Division

Keywords : cryogenics, cooling loop, components, spacing, cost saving

---

Summary :

The Large Hadron Collider (LHC), currently under construction at CERN, will make use of superconducting magnets operating in superfluid helium below 2 K. The reference cryogenic distribution scheme was based, in each 3.3 km sector served by a cryogenic plant, on a separate cryogenic distribution line which feeds elementary cooling loops corresponding to the length of a half-cell (53 m). In order to decrease the number of active components, cryogenic modules and jumper connections between distribution line and magnet strings, a simplified cryogenic scheme is now proposed, based on cooling loops corresponding to the length of a full-cell (107 m) and compatible with the LHC requirements. Performance and redundancy limitations are discussed with respect to the previous scheme and balanced against potential cost savings.

TABLE OF CONTENTS

LIST OF FIGURES

LIST OF TABLES

1. Introduction

The "Yellow Book" (YB) [1] presents a cryogenic scheme consisting of a chain of virtually identical units, thus providing, for maximum standardization, identical layout of functional components (Bus-bar plugs, cooldown and fill valves, safety relief valves, 1.8-K cooling loop components, etc.) at all connections between the distribution line and the accelerator. Figure 1 shows the YB cooling scheme. This cooling scheme has been implemented in Test String 1 [2] and validated in quasi full-scale geometry, and is therefore fully adequate for the LHC.

Following a memorandum [3] by Ph. Lebrun, a working group on Simplified Scheme of Cryogenics (SSC) has been constituted with the following mandate:

- Study of the possibility of reduction of the number and types of components and cryogenic circuits of LHC arcs, in particular by increasing the spacing of technical modules feeding the different cryogenic circuits of the magnet string.

- Identification of critical components and dimensions in order to formulate minimum proposals compatible with technical requirements of LHC.

- Evaluation of potential cost savings of each proposal, balancing them against corresponding performance limitations and reliability losses.

The SSC (Simplified Scheme of Cryogenics) Working Group has studied the possibility for reducing the number of functional components, the suppression of which leads to major cost saving, while losing the standardization of the YB version.

These simplifications concern the following subjects:

- Suppression of header A
- Spacing of tight plugs on bus-bars
- Spacing of cooldown and fill valves
- Length of 1.8-K cooling loops
- Spacing of safety relief valves
- Layout of beam-screen cooling loops
- Spacing of vacuum barriers

The proposals made here remain fully compatible with the recommendations of the Sub-sectorization Working Group [4]. However, implementation of all recommendations of this Working Group requires a higher number and more types of components. The decision to do so still remains open.

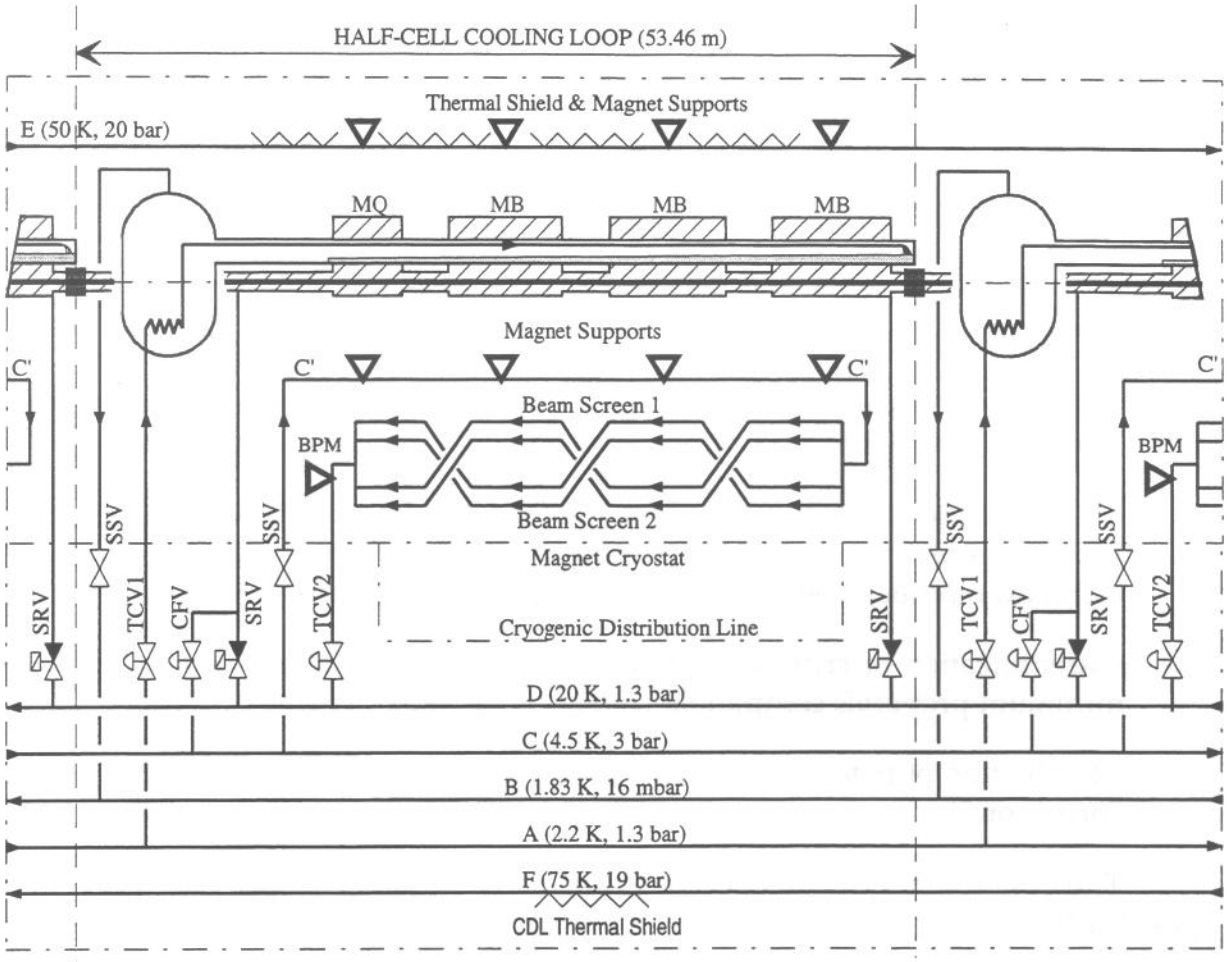

Figure 1: Half-cell cooling loop of the YB version

2. Suppression of header A

2.1. Cooling performance

In order to reduce the vapour mass fraction produced in the Joule-Thomson expansion of the superfluid cooling loop, a subcooled helium supply is required. This subcooling can be performed centrally in the cold compressor box of the corresponding sector (Yellow book version) or distributed in the technical service module of each half-cell (this alternative). The first case requires a single heat exchanger for the total flow of 120 g/s and a subcooled liquid helium header (Header A) in the cryogenic distribution line. In the second case, header A disappears but one smaller heat exchanger in each cooling loop is needed. Figure 2 shows the two subcooling schemes with either central or distributed subcooling heat exchangers.

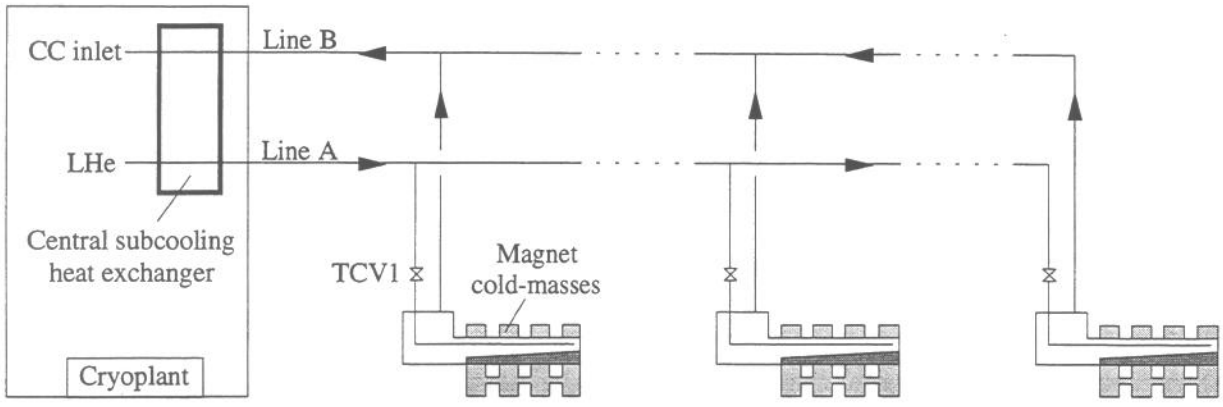

Central heat exchanger scheme

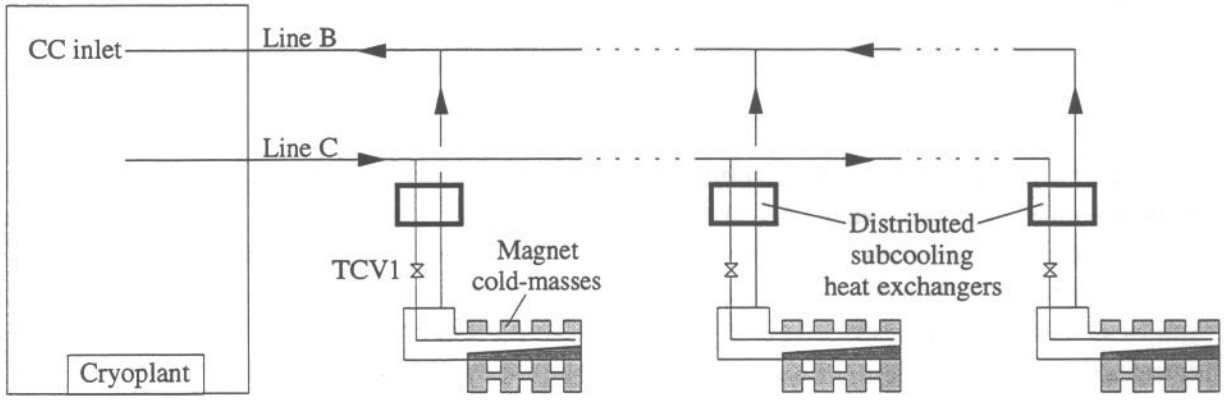

Distributed heat exchanger scheme

Figure 2: Subcooling schemes with central and distributed heat exchangers

The major difference between these two cases is the operating conditions of the pumping header B. Frictional pressure drop is proportional to the gas density and hydrostatic head is inversely proportional to the gas density. In the first case (central heat exchanger), VLP vapour is pumped at 1.8 K, when it is dense, which minimizes frictional losses due to the pumping mass-flow. In the second case (distributed heat exchangers), VLP helium is returned to the CCB at higher temperature, thus reducing hydrostatic head.

The second difference between the two cases is the subcooling performance, which depends, for a given value of heat exchanger efficiency, on the subcooled helium pressure and on the inlet temperature conditions. In order to achieve good performance, the subcooled helium pressure and the VLP inlet temperature must be as low as possible. With a central heat exchanger, the performance is reduced by the higher inlet temperature of the VLP helium which is heated by the heat inleaks falling onto the 3.3-km header B. With distributed heat exchangers, the performance is reduced by the high pressure of subcooled helium which is supplied by header C. Table 1 gives the heat exchanger performance comparison for the installed mode. The vapour fraction produced during expansion in TCV1 valves is similar; the higher inlet temperature with central heat exchanger is about compensated by the higher pressure of subcooled helium.

Table 1: Heat exchanger performance

Case	P HP [bar]	Tin VLP [K]	Tout HP [K]	Gas fraction [%]
Central heat exchanger	1.3	2.4	2.6	17.3
Distributed heat exchanger	3	1.8	2.17	17.5

Figure 3 and Figure 4 show the magnet temperature profiles with central and distributed heat exchangers. Figure 5 and Figure 6 give the allocation of temperature difference for the warmest magnet, which in both cases is in the vicinity of point 5. The magnet temperature is determined by frictional pressure drop in header B, hydrostatic head due to elevation difference, pressure drop in subcooling heat exchangers and temperature difference across the He II heat exchanger tubes in the cold mass.

With distributed heat exchangers, the hydrostatic head is lower but cannot compensate the increase in frictional pressure drop. The warmest magnet temperature undergoes an increase of 22 mK for installed conditions and only 13 mK for nominal conditions. The increase of the warmest magnet temperature is the major drawback of distributed heat exchangers. However, it should be noted that in nominal conditions, the warmest magnet temperature remains at the specified 1.9 K. Table 2 summarizes the advantages of the two solutions.

Table 2: Advantages of central and distributed subcooling heat exchangers

Central heat exchanger	Distributed heat exchangers
Lower temperature of warmest magnet	Suppression of header A
Design pressure of HP stream	Decrease of global heat loads
Working pressure of HP stream	Weaker influences of header B heat loads
Smaller number of heat exchangers	Validation of design and construction

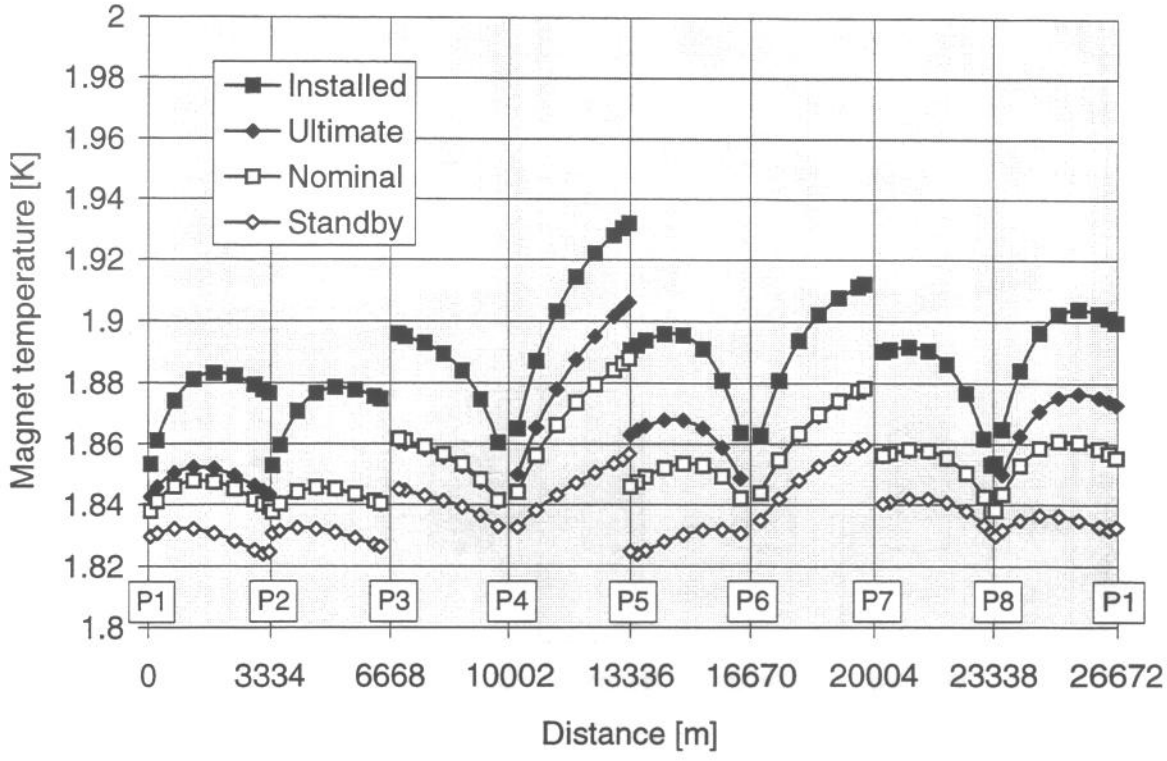

Figure 3: Magnet temperature profile with central heat exchanger

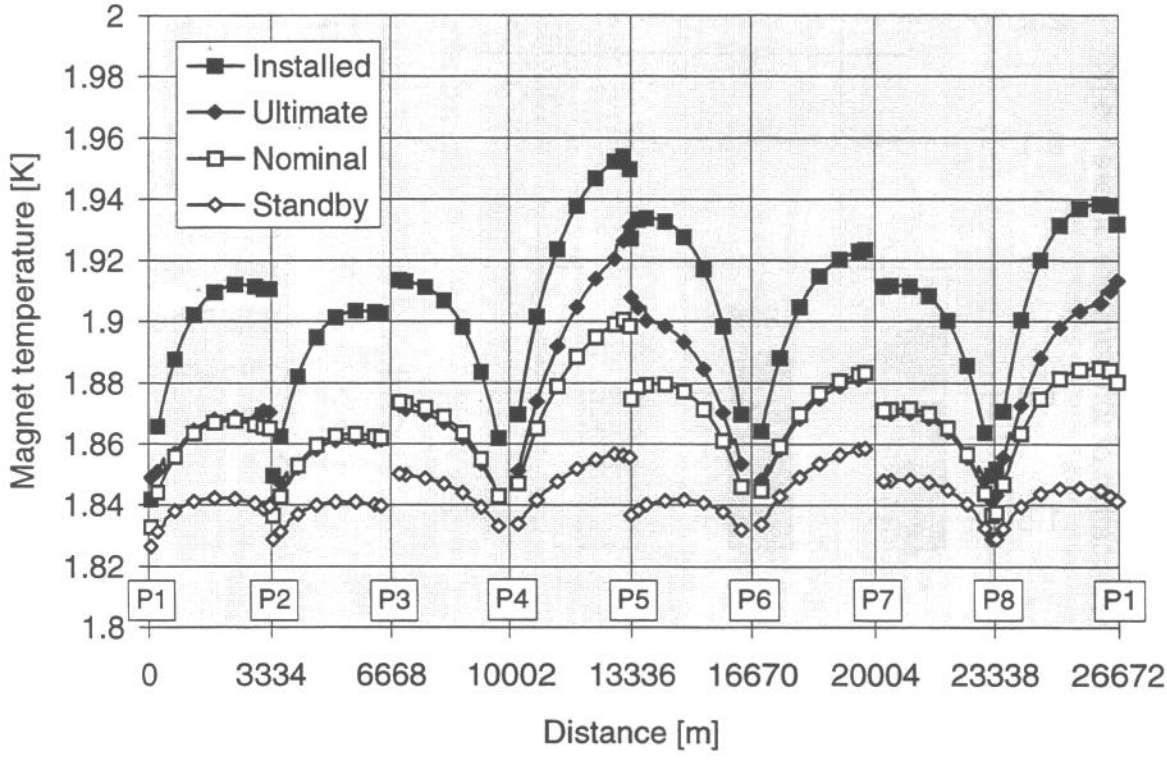

Figure 4: Magnet temperature profile with distributed heat exchangers

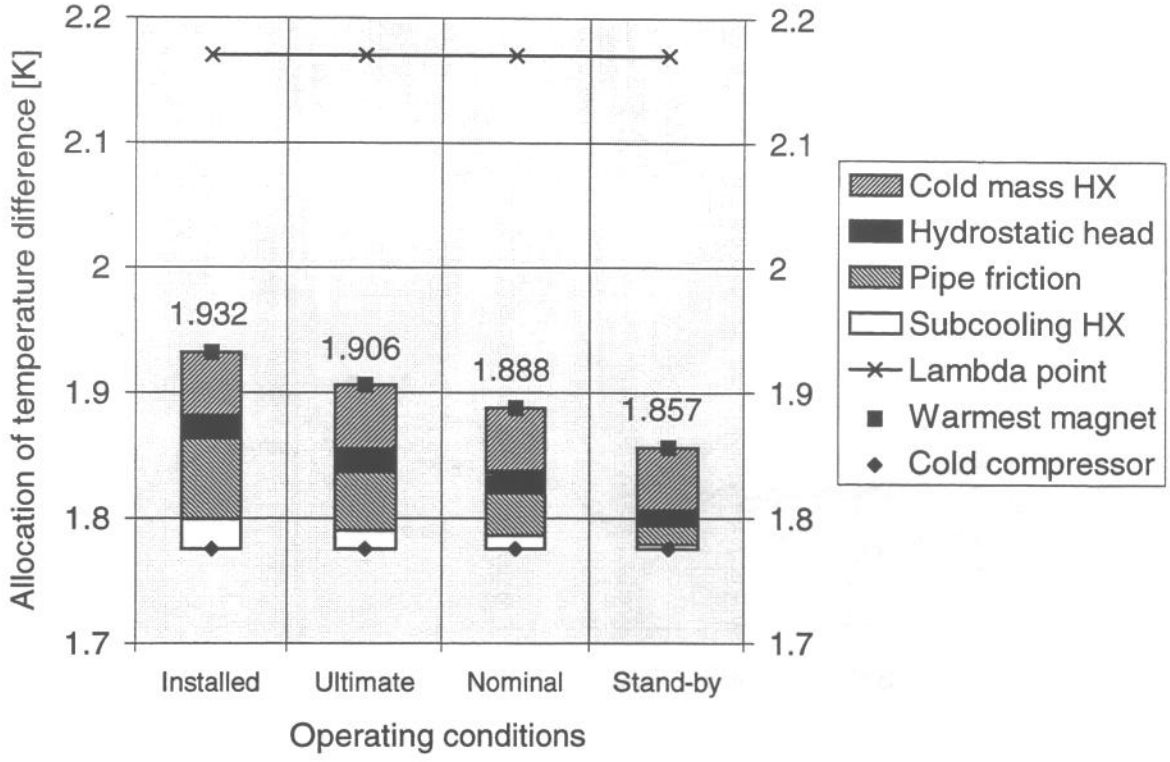

Figure 5: Allocation of temperature difference with central heat exchanger

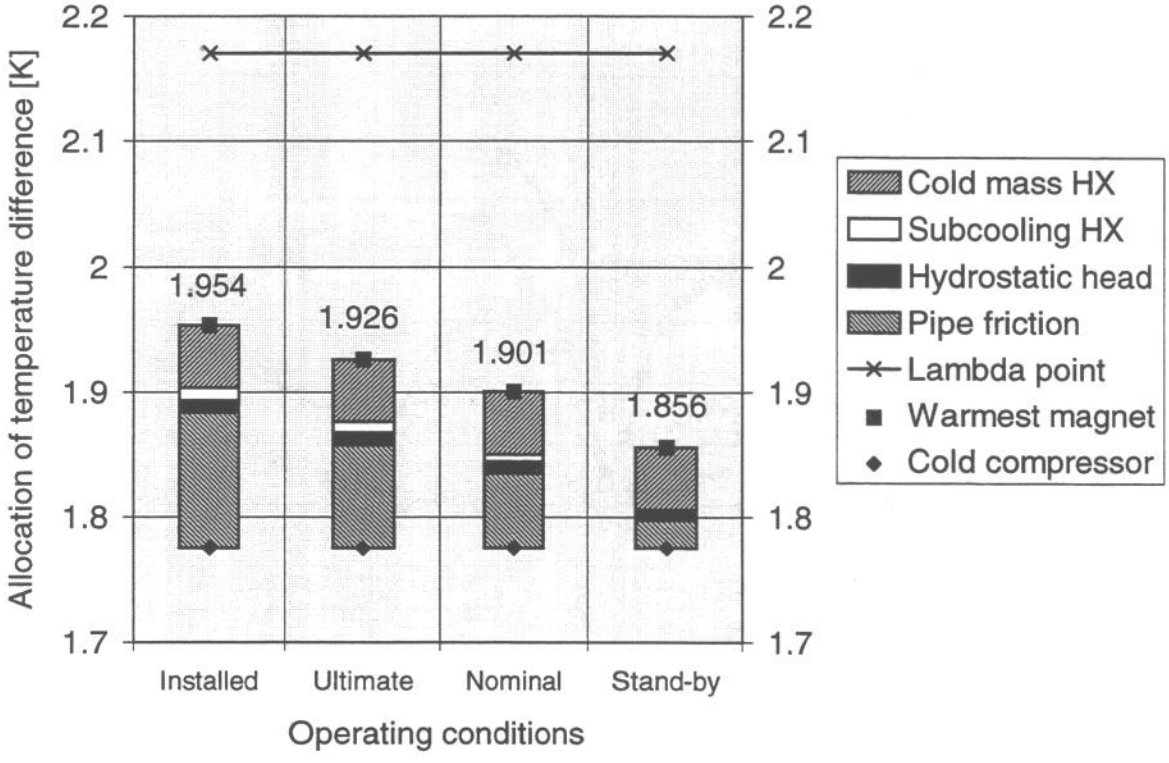

Figure 6: Allocation of temperature difference with distributed heat exchangers

2.2. Sizing of distributed heat exchanger

Table 3 gives the static and dynamic heat loads and the corresponding installed power per cooling loop with and without collimation losses. Without collimation losses, the installed power is determined by nominal conditions. Adding the collimation losses, the installed power is determined by injection at nominal energy. Taking into account the collimation losses, the installed power increases by 33 % (for a half-cell loop) and 11 % (for a full-cell loop) with respect to those without collimation losses. For full-cell cooling loops, the collimation losses do not influence drastically the necessary size of the distributed heat exchangers.

Table 3: Installed power per cooling loop

Cooling loop	Mode	Q static	Q dynamic w/o collimation losses	Q Installed w/o collimation losses	Collimation losses	Q installed with collimation losses
		[W]	[W]	[W]	[W]	[W]
Half-cell	Standby	14.4	0	27	0	27
	Inj. nominal	14.4	5.7	35.5	12	**53.5**
	Inj. ultimate	14.4	5.7	23.7	19	42.7
	Nominal	14.4	8.8	**40.2**	3.4	45.3
	Ultimate	14.4	8.1	26.1	5.4	31.5
Full-cell	Standby	28.8	0	54	0	54
	Inj. nominal	28.8	11.4	71.1	12	**89.1**
	Inj. ultimate	28.8	11.4	47.4	19	66.4
	Nominal	28.8	17.6	**80.4**	3.4	85.5
	Ultimate	28.8	16.2	52.2	5.4	57.6

Existing designs of subcooling heat exchangers have a capacity in the 2 to 6 g/s range. The feasibility of central heat exchangers, having a capacity of 120 g/s, is not established and their development and technological validation are by no means trivial. The only difficulty of distributed heat exchangers, connected to header C, is that they must have a design pressure of 20 bar on the high-pressure stream to cope with cooldown and warmup conditions.

Table 4 gives the design requirements, that have to be fulfilled by central and distributed heat exchangers.

Table 4: Requirements of central and distributed heat exchangers

Heat exchanger requirements		Distributed		Central
		Half-cell	Full-cell	
Mass-flow	[g/s]	2.7	4.5	120
Inlet HP pressure	[bar]	2.4 to 3.6	2.4 to 3.6	1.5
Inlet HP temperature	[K]	4.6 to 4.9	4.6 to 4.9	2.9
Inlet VLP pressure	[mbar]	16.4 to 19.5	16.4 to 19.5	16
Inlet VLP temperature	[K]	1.8 to 1.85	1.8 to 1.85	2.4
VLP pressure drop	[mbar]	≤ 1	≤ 1	≤ 1
Outlet HP temperature	[K]	≤ 2.2	≤ 2.2	≤ 2.6
HP pressure drop	[mbar]	< 200	< 200	< 100
Maximum HP pressure	[bar]	20	20	6
Maximum VLP pressure	[bar]	6	6	2
Number per arc	[-]	54	27	1

2.3. Recommendation and open issues

The suppression of header A is recommended for the simplified scheme.

Concerning central heat exchangers, the feasibility of such components with good efficiency is not yet established and would require a heavy R&D programme.

Concerning distributed heat exchangers, the high-pressure phase must operate with supercritical helium close to the critical point (supply by header C at 3 bar). In such conditions, pressure and temperature instabilities could appear and affect the heat exchanger efficiency. Studies are under way to understand these phenomena.

3. Spacing of bus-bar plugs and CFVs

3.1. Requirements of short interventions

When the machine is cold, it must be possible to warm-up a limited section of the machine as fast as possible for a local intervention. Such an intervention - called "short" intervention - is useful to remove cold-mass components like for example cold diodes, without removing a complete cryomagnet from the tunnel.

During this short intervention, the helium vessel of the cold mass is open and linked to the air. To avoid circuit pollution by air, tight bus-bar plugs are required. As the magnet vacuum enclosure is open to atmosphere, to avoid frost on interconnection lines, additional part of the machine, staying under vacuum, has to be warmed up as thermal guard. Figure 7 shows the machine configuration during a short intervention.

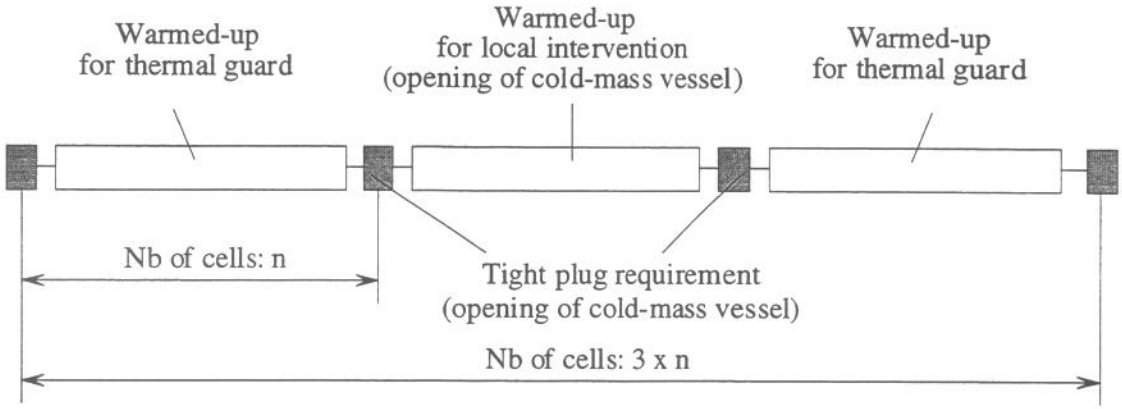

Figure 7: Configuration of cold mass during a short intervention.

In warm-up and cooldown mode, the maximum gaseous helium flow per cell is limited to 100 g/s and the total available flow per sector is limited to 770 g/s. If n is the number of cells between two tight plugs, the total number of cells to be warmed up is thus 3n. To avoid losing time during cooldown and warmup, the following condition has to be verified.

$$3 \cdot n \cdot 100 \leq 770 \Rightarrow n \leq 2.57$$

In order to make the most of short interventions, tight plugs are required every 2 or 3 cells. Figure 8 shows the plug spacing as required for short intervention. The minimum requirement for short intervention is tight bus-bar plugs in 12 locations.

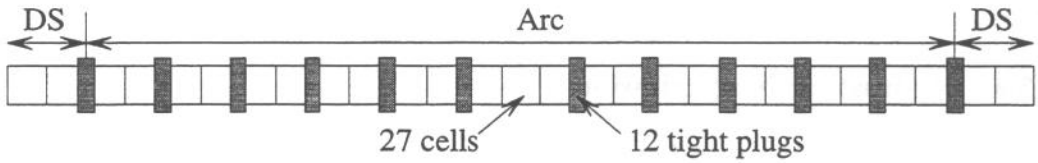

Figure 8: Plug spacing as required for short intervention

3.2. Requirements of cryomagnet removal

The possibility of exchanging a cryomagnet without warming up of the complete sector has to be taken into account. To achieve this, the Sub-sectorization Working Group recommended 4 sub-sectors.

To remove a cryomagnet, interconnection lines and vacuum enclosures are open to the atmosphere. To avoid circuit pollution by air, tight bus-bar plugs are required. To avoid frost on interconnection lines, one extra cell staying under vacuum has to be warmed up as thermal guard. Restrictions are required to limit heat and helium exchange between this cell and the remaining cold part. Figure 9 shows the plug spacing for magnet removal. The minimum requirement for magnet removal is 6 tight plugs and 6 restrictions.

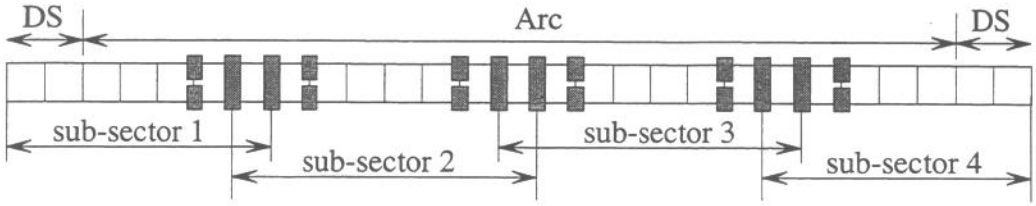

Figure 9: Plug spacing as required for magnet removal

3.3. Combined requirements

Short interventions and cryomagnet removal lead to different requirements for spacing of the bus-bar plugs. It is however possible to combine both requirements. Figure 10 shows a plug spacing, which fulfills the requirements of both types of interventions: 14 tight plugs are required, i.e. 2 additional plugs with respect to the short intervention requirements. With the combined requirement, in case of magnet removal, one or two additional cells for thermal guard have to be warmed up. The corresponding warmup duration will increase from 10 to 20 %.

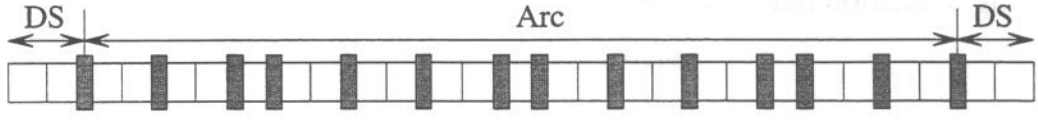

Figure 10: Plug spacing for combined requirement

Instead of fifty-three plugs in the YB scheme, fourteen tight plugs are now required.

3.4. Hydrostatic head criterion

A maximum cold-mass length of 214 m without plug, results from the plug spacing defined above. Taking into account a maximum tunnel slope of 1.4 % and an average superfluid helium density of 148 kg/m^3, the maximum elevation difference is 3 m and the corresponding hydrostatic head is 4.3 kPa (43 mbar). Depending on the normalization point with respect to the header D at a pressure of 1.3 bar, the cold-mass pressure varies from 1.257 to 1.343 bar. This pressure variation is compatible with minimum cold-mass pressure (> atmospheric pressure) and residual leakage across safety relief valves.

3.5. Quench propagation criterion

Different modes of quench propagation could occur from magnet to magnet:

- propagation in bus-bars by resistive heating, which can traverse a plug,
- propagation by convection of warm helium, which is stopped by a plug.

Irrespective of the quench propagation mechanism, a limit can be derived from the simple argument that, due to current decay after 100 s, the current level of the magnet is low enough to avoid quenches. Figure 11 shows the number of quenched magnets versus the quench propagation time. On the Test String, measurements give a propagation time of 50 seconds per magnet, which maintains the propagation within one or two cells (depending on the starting point). This propagation was

measured from quadruple to dipole and the level of deposited energy was very low. In case of dipole to dipole propagation, the propagation time will probably be lower.

For the LHC, in case of a limited quench, the number of quenched cells must remain below 4. This number is based on reasonable recooling time after a quench and on limiting the number of temperature cycles undergone by magnets. For quenches of 4 cells, the propagation time should be faster than 6 seconds per magnet. Results from the Test String show that this is very unlikely.

The maximum number of cells involved in a limited quench can then be safely estimated to below 4. This number will be revised after better understanding of quench propagation phenomena.

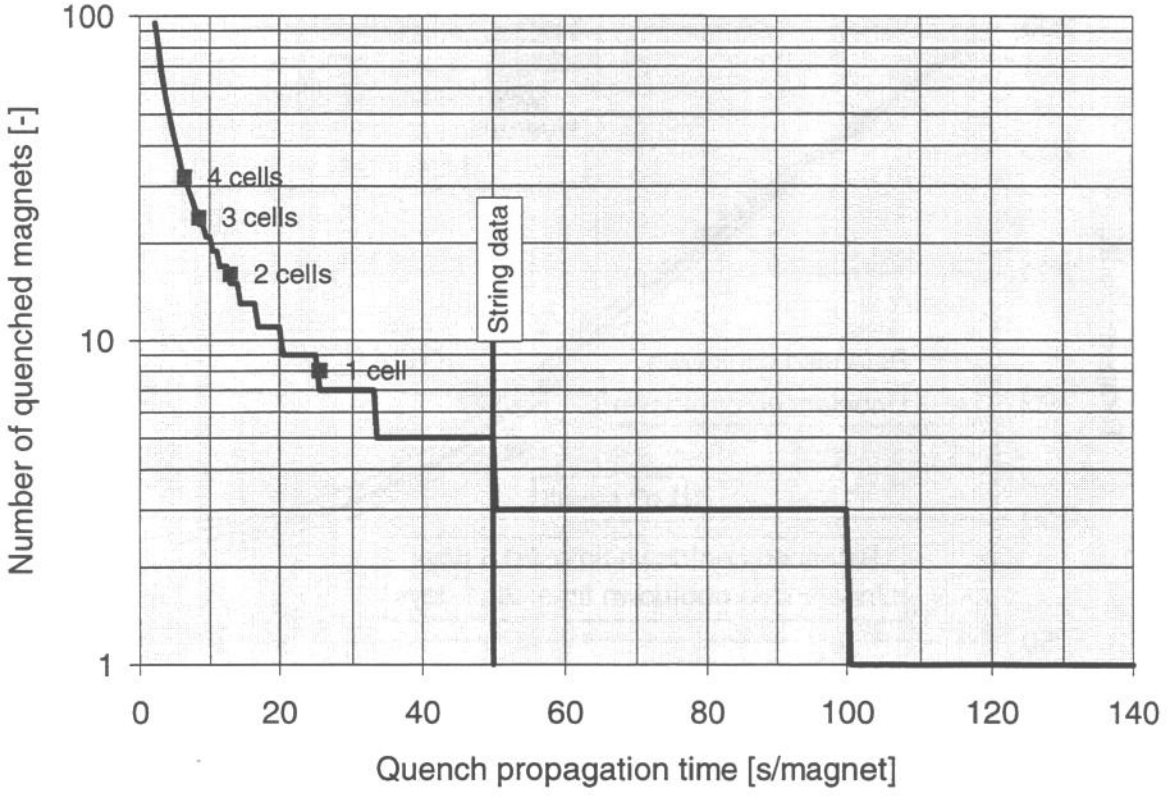

Figure 11: Number of quenched magnets versus propagation time

3.6. Forced-flow cooldown and warmup criterion

To avoid high gas velocity in magnets and to limit the pressure drop, the maximum length of magnets to be cooled in series corresponds to one cell. Figure 12 shows two circuit configurations with series and parallel arrangement. In case of series arrangement, additional restrictions (12 per arc) are needed. Parallel arrangement requires no additional devices, but the flow balance and consequently the cooldown time depends on hydraulic impedance and mass to be cooled in the two parallel circuits. Differences of 20 % on the hydraulic impedance and 5 % on the mass yield an increase in cooldown time of 10 %. This unbalance could be corrected by pulse duration modulation type control of the outlet valves (safety relief valves). Figure 13 shows a parallel cooldown with balanced and unbalanced circuits.

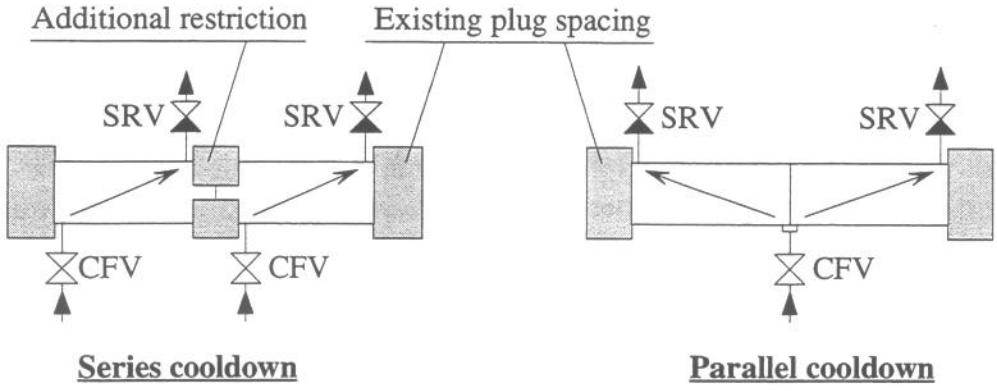

Figure 12: Circuit arrangements for cooldown and warmup

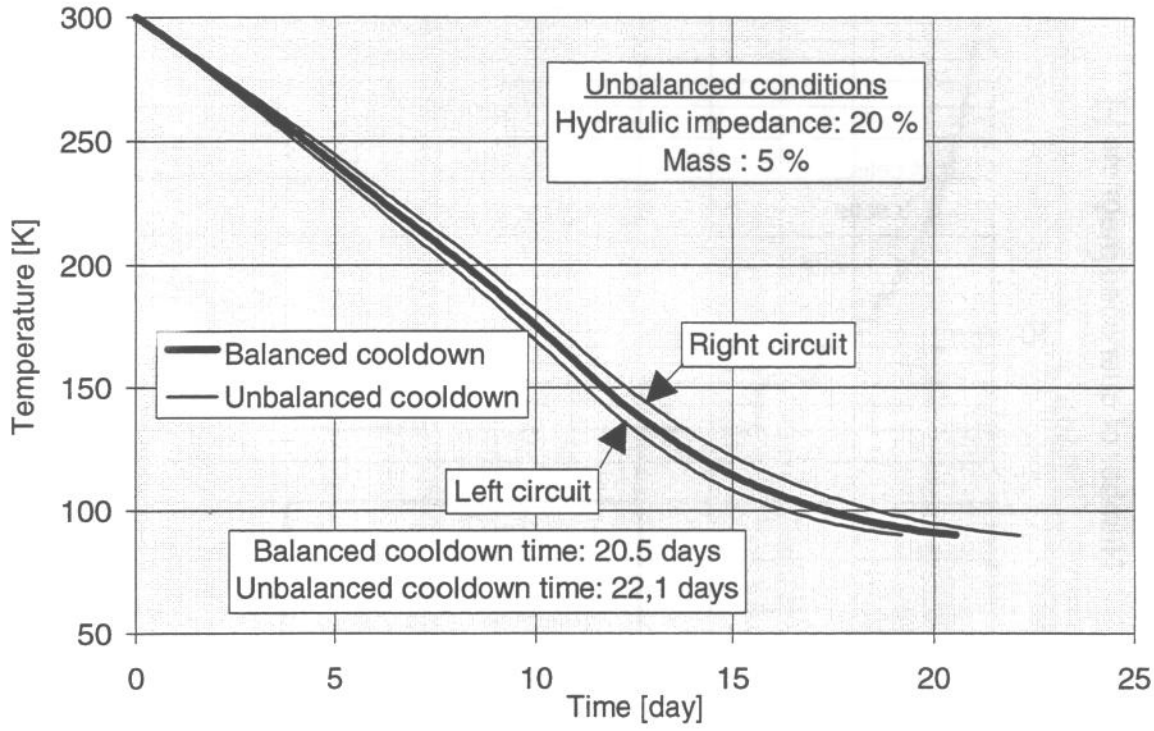

Figure 13: Cooldown time with parallel arrangement

The parallel arrangement is compatible with efficient cooldown and avoids additional CFV's and restrictions. This arrangement is recommended for the simplified scheme. The series arrangement is still required at three places for the overlapping cells of sub-sectors.

3.7. CFV spacing and sizing

Cooling and fill valves (CFV), which feed parallel circuits, see higher flows than in the YB layout. Figure 14 shows the CFV valve spacing and Table 5 gives the CFV operating conditions with the corresponding flow coefficient Kv and nominal diameter DN. The cryomagnet removal intervention requires a DN32 valve for parallel feed.

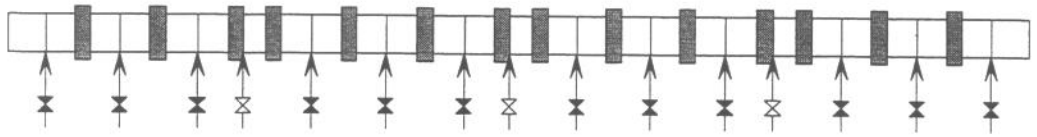

12 parallel-feed valves and 3 series-feed valves

Figure 14: CFV valve spacing

Instead of 54 series-feed valves in the YB scheme, a minimum of 12-parallel-feed and 3-series-feed valves are now required.

Table 5: CFV operating requirement and sizing

Characteristics	Series feed		Parallel feed	
	Magnet removal	Fast sector cooldown	Magnet removal	Fast sector cooldown
Mass-flow [g/s]	90	60	180	120
Inlet pressure [MPa]	0.9	1.15	0.9	1.15
Outlet pressure [MPa]	0.85	1.1	0.85	1.1
Kv [m3/h]	14	8.5	28	17
DN [mm]	25 *	20 *	32 *	25 *

* can vary depending on the valve supplier

3.8. Recommendation and open issues

The plug and CFV spacings, given in Figure 14 are recommended for the simplified scheme.

One "plug" as defined in this study represents, in reality, 4 tight feedthroughs on each of the 4 bus-bar connection pipes between cold-masses. Short and magnet-removal interventions require tight plugs with a leak rate similar to an isolation valve, i.e. better than 10^{-3} mbar.l/s. Such plugs have not yet been designed and some uncertainties on their feasibility and cost are still existing.

4. He II cooling of the cold-mass

4.1. Cooling mode

In the YB, the reference principle of magnet string cooling is based on a DHP corrugated heat exchanger with co-current two-phase flow of saturated He II. One technical variant studied and tested in the Test String is counter-current two-phase flow. Operating the two-phase helium II heat exchanger tube in counter-current flow of liquid and vapor would bring complete symmetry in the cryogenic layout of the half-cell cooling loop, independent of the tunnel slope. However, counter-current has shown strong flow-blocking limitation ("flooding") [5].

In counter-current flow, scaling from string measurements gives a maximum deposited power per loop that can be extracted of 60 W, i.e., a maximum distributed

power of 1.2 W/m for a half-cell cooling loop and only 0.6 W/m for a full cell cooling loop, which corresponds to a maximum mass-flow of 3 g/s. Comparing these values with the installed power of 0.75 W/m (without collimation losses), and with the required flow of 12 to 24 g/s for fast recooling after a limited quench, shows that counter-current flow is not compatible with both half- and full-cell cooling. Moreover, no experimental data for fully horizontal flow are available today.

The co-current flow is therefore the only possible choice for LHC and will be considered in the following. The helium supply and pumping, and consequently the arrangement of the cryogenic technical module in the Short Straight Section unit, depend on the slope. Singularities for the lowest and highest points, where the slope changes, also increase the functional number of different types of modules.

The cold mass heat exchanger is used to extract the heat load on the cold mass. Figure 15 shows the heat exchanger scheme with the temperature at the different locations. The total temperature difference across this heat exchanger, which should remain below 50 mK, depends on the following terms:

- Heat exchanger pressure drop ($\Delta T1 = Ts1 - Ts0$)
- Kapitza resistance on saturated He II side ($\Delta T2 = Tscu - Ts$)
- Solid conduction across copper wall ($\Delta T3 = Tpcu - Tscu$)
- Kapitza resistance on pressurized He II side ($\Delta T4 = Tp - Tpcu$)
- Partial dry-out of heat exchanger ($\Delta T5 = 10$ mK)
- Precision on temperature measurement on pressurized He II ($\Delta T6 = \pm 10$ mK)
- Precision on temperature measurement on saturated He II ($\Delta T7 = \pm 5$ mK)
- Control loop ripple and overshoot ($\Delta T8 = 15$ mK)

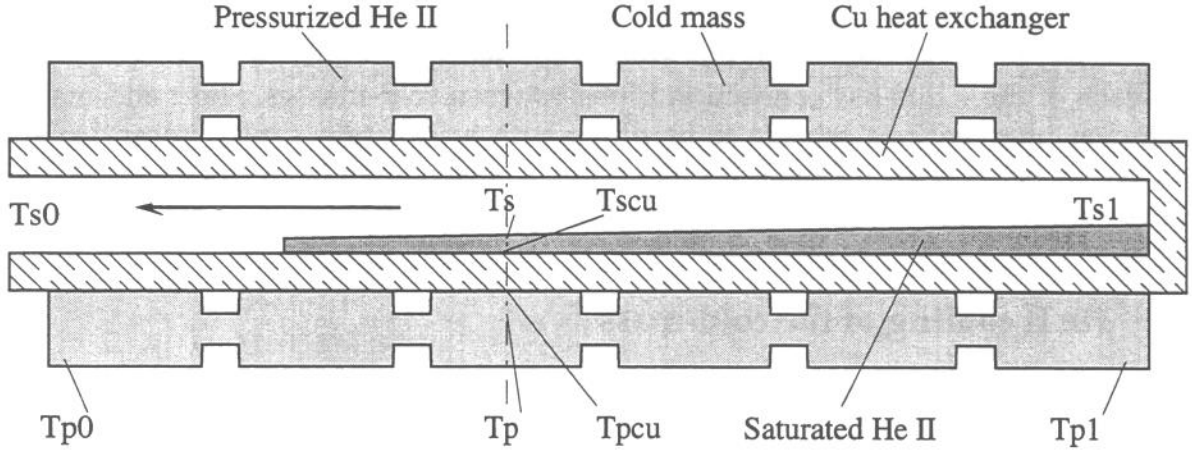

Figure 15: Heat exchanger scheme showing temperature at different locations.

The maximum value of Tp0 is given by:

$$Tp0 = Ts0 + \Delta T2 + \Delta T3 + \Delta T4 + \Delta T5 + |\Delta T6| + |\Delta T7| + \Delta T8$$

The maximum value of Tp1 is given by:

$$Tp1 = Ts0 + \Delta T1 + \Delta T2 + \Delta T3 + \Delta T4 + \Delta T8$$

Depending of the relative value of $\Delta T1$ and ($\Delta T5$ + $|\Delta T6|$ + $|\Delta T7|$), the maximum temperature in the pressurized helium is either Tp0 or Tp1.

4.2. Inner supply pipe

Co-current flow imposes to supply helium at the higher point of the loop and a supply pipe is therefore needed. To avoid additional heat inleak and to reduce risk of helium leaks, this pipe is placed in the cold-mass heat exchanger. An advantage of this arrangement is the increase in frictional pressure drop in the liquid flow, yielding a lower velocity and thus better wetting of the tube wall for a given liquid flow-rate. A drawback of this arrangement is the increase of frictional pressure drop in the vapour flow. Figure 16 shows the pressure drop ratio as compared with an empty tube. In the YB version, the corresponding ratio is 1.66 (d/D= 0.29). In the new scheme, the 1.9 K cooling loop is supplied by the header C at a pressure of 0.3 MPa (instead of 0.13 MPa in the YB version). This increase of supply pressure allows to reduce the inner pipe diameter. Figure 17 shows the pressure drop in the inner supply pipe. In case of recooling after a limited quench, an inner diameter of 10 mm is sufficient and the corresponding pressure drop ratio is 1.5 (d/D= 0.24). This reduction with respect to the YB value is linked to the suppression of header A. If the header A were maintained, an inner diameter of 12 mm would be required as in the YB version.

For the installed capacity, with an inner diameter of 10 mm, the corresponding pressure drop is 27 mbar (see Figure 17). This pressure drop creates a temperature difference between helium in the supply pipe and in the cold-mass heat exchanger. The supply pipe therefore performs as a partial reliquefier of the vapour fraction, thus reducing the pressure drop in the cold mass heat exchanger.

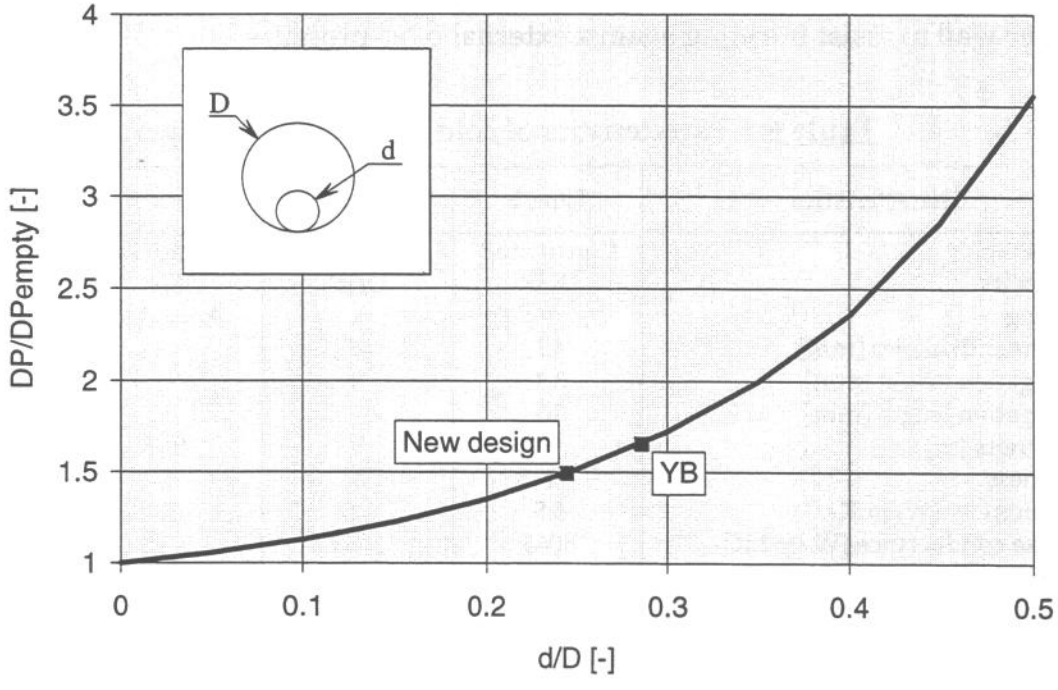

Figure 16: Pressure drop in tube with cylindrical obstruction, with respect to an empty cylindrical tube.

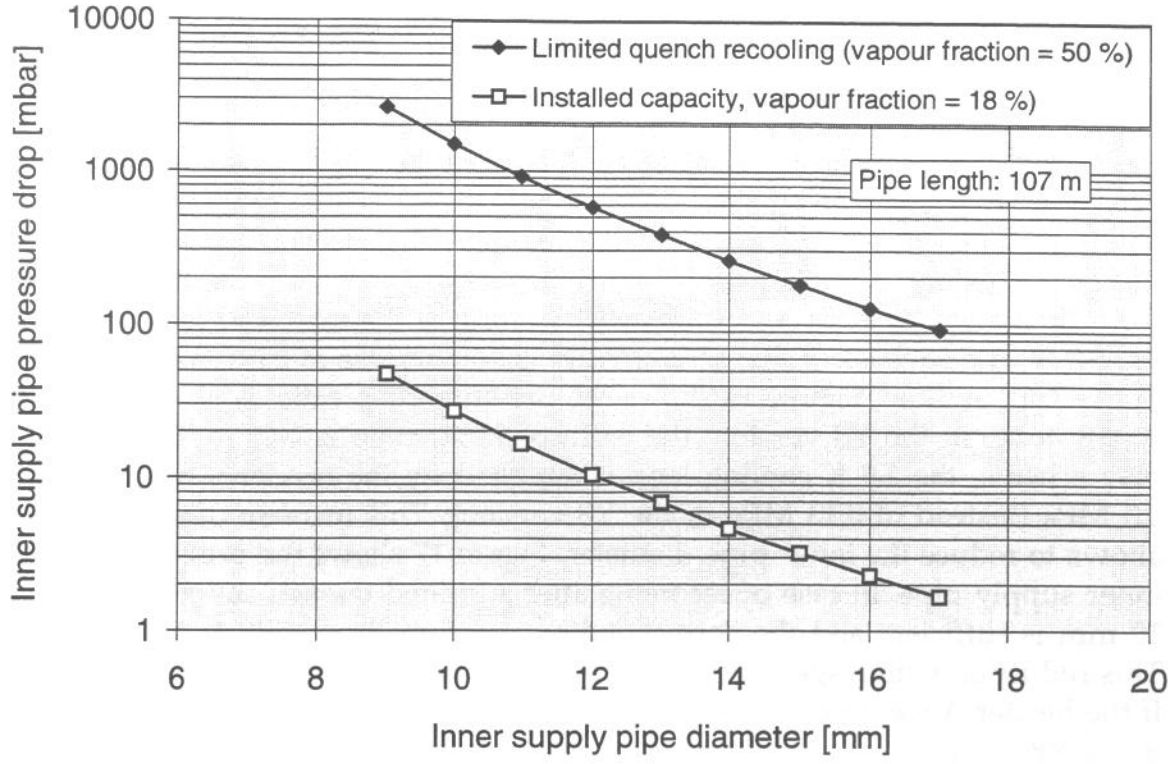

Figure 17: Pressure drop in inner supply pipe.

4.2. Heat exchanger design

Table 6 gives the characteristics of the cold-mass heat exchanger. Four types of heat exchanger are envisaged: corrugated tube in DHP copper quality and cylindrical tube in DHP or OFHC copper quality. The cylindrical type requires a thicker wall to resist buckling against external over-pressure.

Table 6: Characteristics of cold mass heat exchanger.

Characteristics	Type 1	Type 2	Type 3	Type 4
Tube shape	Corrugated	Cylindrical	Cylindrical	Cylindrical
Cu quality	DHP	DHP	OFHC	OFHC
Treating	\	\	Annealed	Cold work
Free inner diameter [mm]	49	49	49	54
Corrugation height [mm]	3.1	\	\	\
Corrugation length [mm]	10	\	\	\
Roughness [m]	\	\	2E-5	2E-5
Thickness	1	4	4	2
Conductivity [W/m.K]	5.5	5.5	30	30
Kapitza conductance [W/m2.K]	5065	5065	5065	5065
Wetted perimeter [mm]	51.3	51.3	51.3	56.6
Overall linear conductance [W/m.K]	89	46	97	122

In calculations, the thickness of the cylindrical tubes of type 2 and 3 is conservatively estimated from CODAP. The type 4 is optimized according to the maximum available space in the yoke passage , taking into account the increase in yield strength due to cold work. The Kapitza conductance is assumed to be

independent of the copper quality. The wetted perimeter is assumed to be independent of tube shape, constant along the tube length and taken at one third of the total perimeter.

Table 7 gives the values of temperature differences for the different types of heat exchanger, and for 53-m and 107-m lengths. The values are given for the linear distributed power of 0.75 W/m (installed conditions without collimation losses).

Table 7: Temperature differences across the cold-mass heat exchanger.

	Type 1		Type 2	Type 3	Type 4
Length [m]	53 (YB)	107	107	107	107
ΔT1 [mK]	11.2	70.4	14.8	14.8	8.8
ΔT2 [mK]	2.9	2.9	2.9	2.9	2.7
ΔT3 [mK]	2.7	2.7	10.6	1.9	0.9
ΔT4 [mK]	2.9	2.9	2.9	2.9	2.7
ΔT5 [mK]	10	10	10	10	10
ΔT6 [mK]	10	10	10	10	10
ΔT7 [mK]	5	5	5	5	5
ΔT8 [mK]	15	15	15	15	15
Tp0-Ts0 [mK]	48.4	48.4	56.4	47.7	46.3
Tp1-Ts0 [mK]	34.6	93.8	46.1	37.5	30.0

Figure 18 shows the maximum temperature differences for the different heat exchanger types. For a length of 107 m, only types 3 and 4 give temperature difference within the allocated budget; types 1 and 2 exceed the budget because of pressure drop ΔT1 (for type 1) and solid conduction across copper wall ΔT3 (for type 2). To preserve performance at least equal to that of the YB, for a length of 107 m, a type 4 heat exchanger with an inner diameter of 54 mm is required. This can be implemented without modification of the passage in the magnet yoke. Table 8 summarizes the main characteristics of the required cold-mass heat exchanger.

Due to use of higher-grade copper, higher mass and possible need for bellows compensators, this new heat exchanger, is more expensive than the corrugated type used in the YB solution.

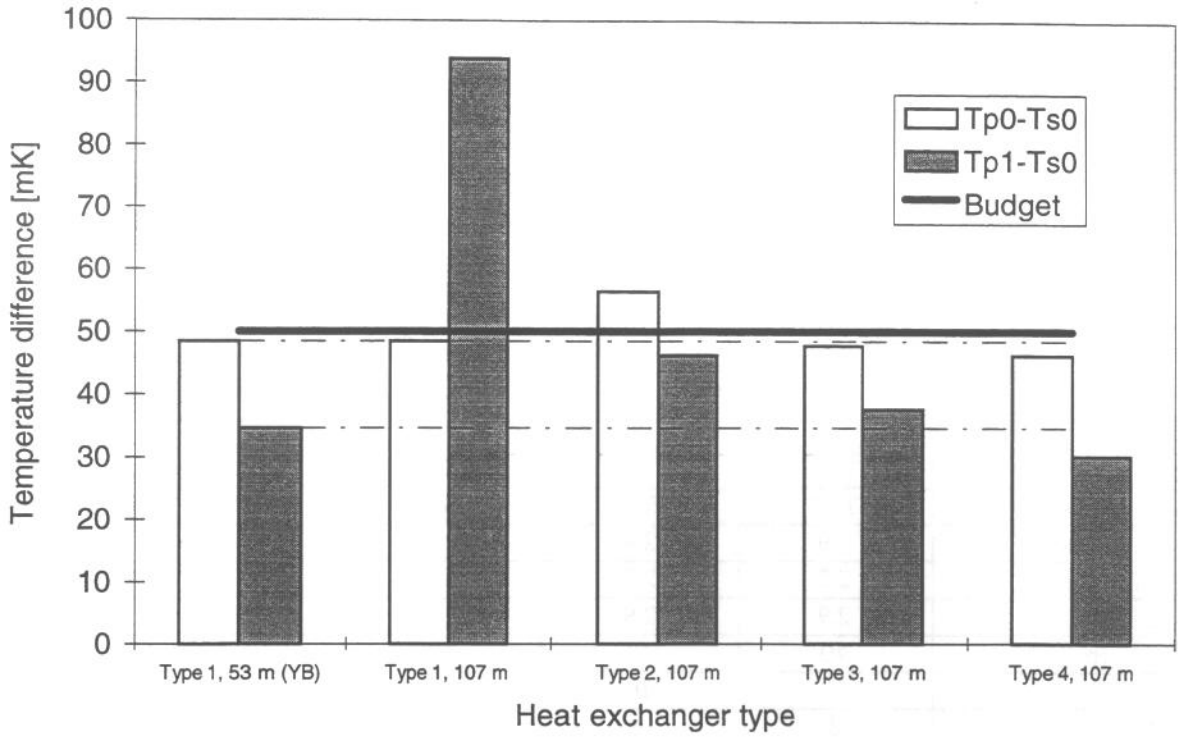

Figure 18: Maximum temperature differences for different heat exchanger types

Table 8: Characteristics of a full-cell cold-mass heat exchanger compatible with the present cold mass design

Characteristics		
Length	[m]	107
Tube shape	[-]	Cylindrical
Cu quality	[-]	OFHC
Cold work treating	[%]	20
Free inner diameter	[mm]	54
Thickness	[mm]	2
Outer diameter	[mm]	58
Yoke passage	[mm]	60
Roughness	[m]	2E-5
Conductivity	[W/m.K]	30
Kapitza conductance	[W/m2.K]	5065
Wetted perimeter	[mm]	57
Overall linear conductance	[W/m.K]	122

4.3. Cooling loop behaviour

Figure 19 shows the working principle of the cooling loop. The He II cooling loop is based on a control of the difference between the pressurized superfluid helium temperature Tp0 and the saturated helium temperature reference Ts0 in the separator sump. This control requires a partial dry-out of the heat exchanger. At the dry-out point, all the liquid is vaporized and the total vapour flow has to be pumped over the remaining length and consequently, with respect to a fully wetted heat exchanger, produces increases of the total pressure drop in the heat exchanger and of the temperature Tsw of the saturated liquid. In addition, the total power reaching the magnet string has to be extracted over a shorter-wetted-length and consequently the difference between the saturated temperature Tsw and the pressurized liquid temperature Tpw is higher. In the remaining part of pressurized helium located after the dry-out point, the heat must be extracted by conduction in static superfluid helium, which creates an additional elevation of temperature.

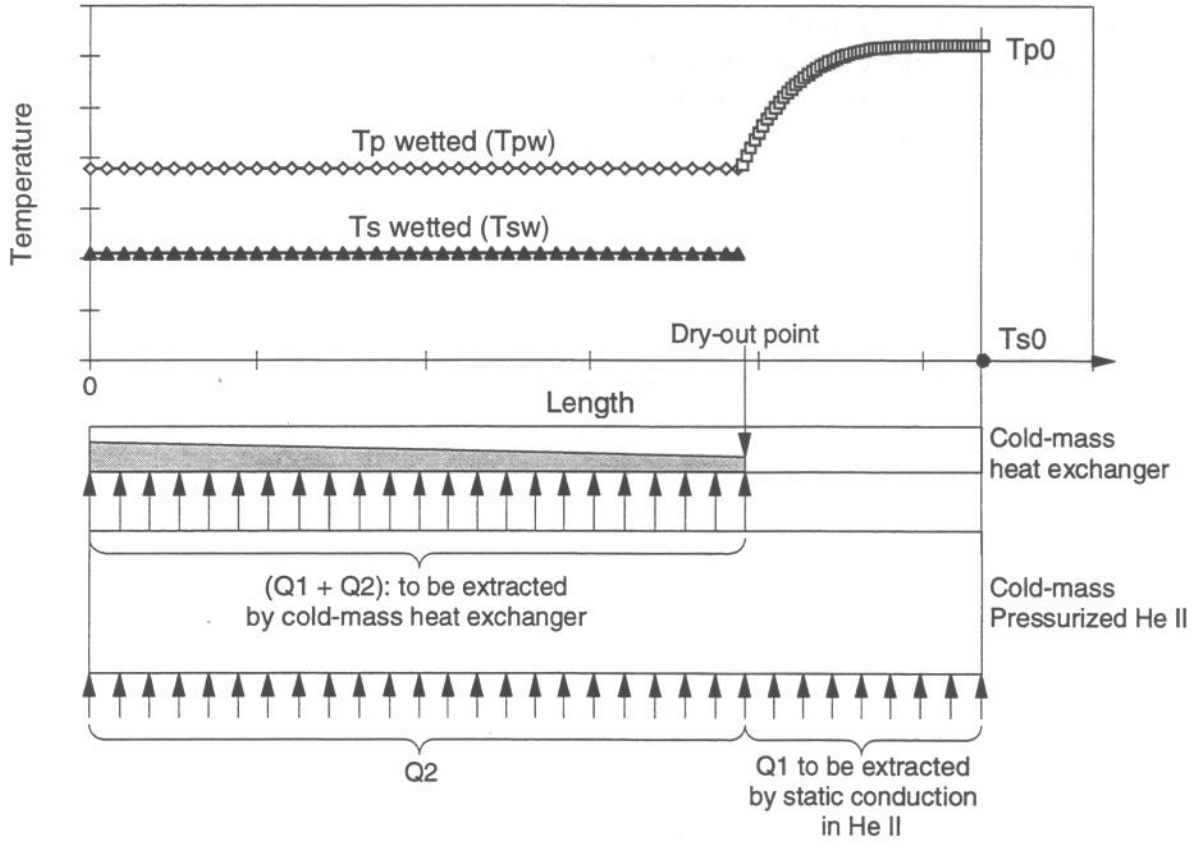

Figure 19: working principle of He II cooling loop

In this type of control, the set-point has to be chosen in order to avoid over-flowing of liquid (in case the set point in temperature difference is set too low), as well as magnet temperature above 1.9 K (in case the set point in temperature difference is set too high). Taking into account the uncertainties on temperature measurements in the saturated and pressurized helium, two forbidden zones can be defined.

Figure 20, Figure 21 and Figure 22 show the average temperature of the saturated liquid (Tsw) and of the magnets (Tpw) as a function of the position of the dry-out point, as well as the two forbidden zones for the following cases:

- The Test String
- A LHC cell with type 3 heat exchanger
- A LHC cell with type 4 heat exchanger

These curves are established for the installed capacity (0.75 W/m) and for a saturated temperature reference of 1.85 K. An "ideal" set-point can be chosen between the two forbidden zones by balancing the remaining temperature margin.

For the Test String, the "ideal" set-point corresponds to 1.88 K, i.e. 30 mK with respect to the saturated temperature reference Ts0. The dry-out point is located at 16 m in the second dipole. This has been experimentally verified, and thus gives confidence in the calculations.

Concerning the LHC cell cooling loop with the type-3 heat exchanger, the "ideal" set point is higher (35 mK with respect to the saturated temperature reference Ts0), and the margin on the temperature is close to zero, i.e. over-flow or too high magnet temperatures may occur in case of transient mode like current ramping. With the present temperature accuracy, type-3 heat exchanger is not suitable.

With type 4 heat exchanger, the cell cooling loop behaviour is similar to that of the Test String, and provides reasonable temperature margin.

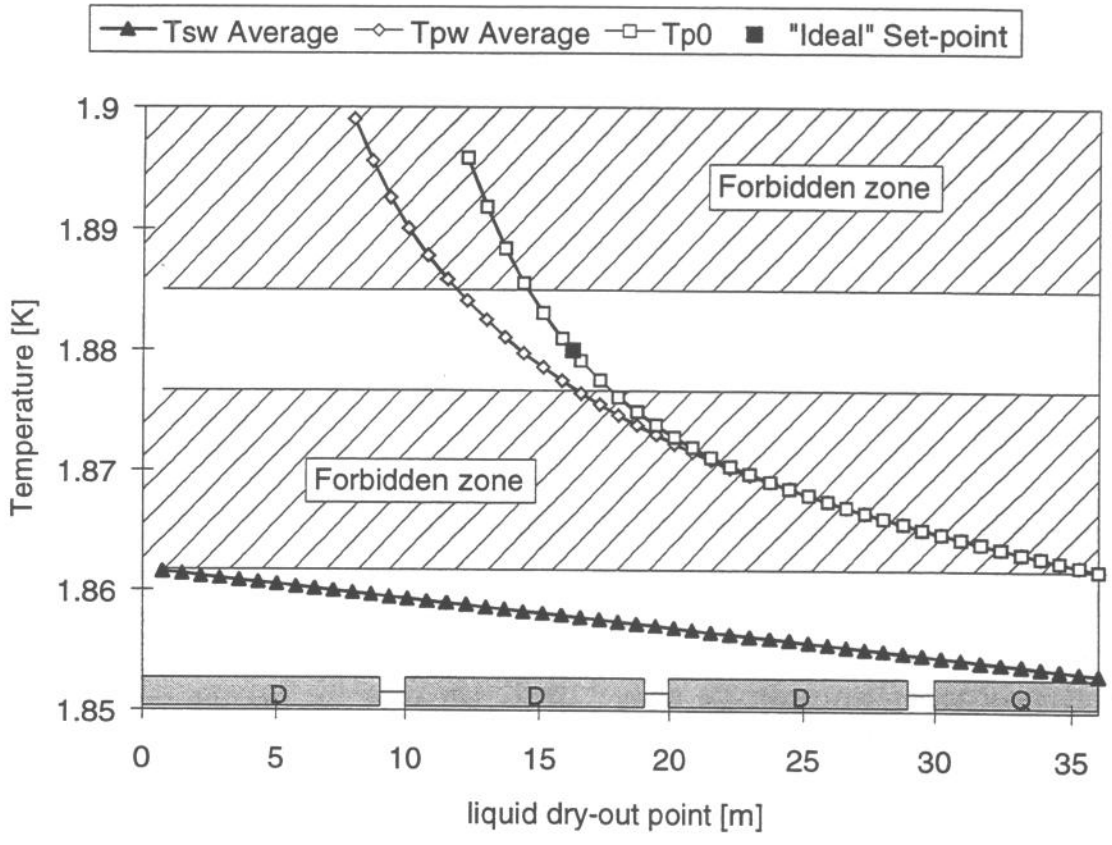

Figure 20: He II cooling loop behavior of the Test String

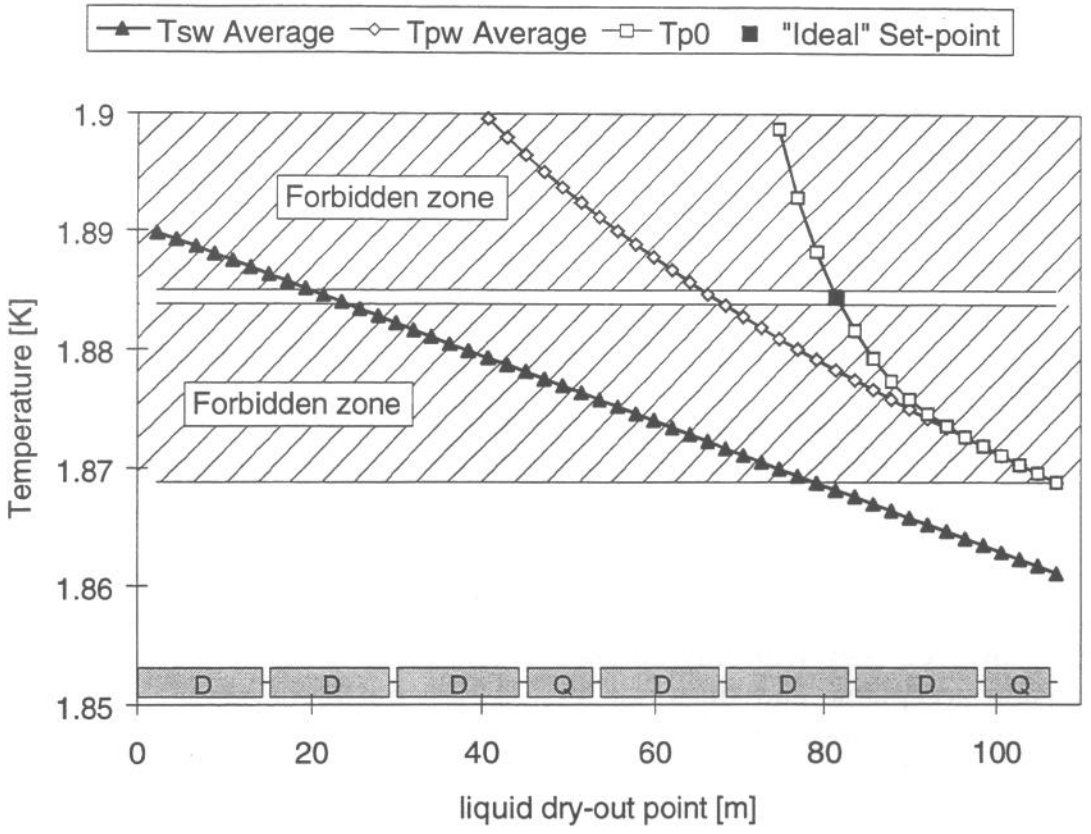

Figure 21: He II cooling loop behavior with type 3 heat exchanger

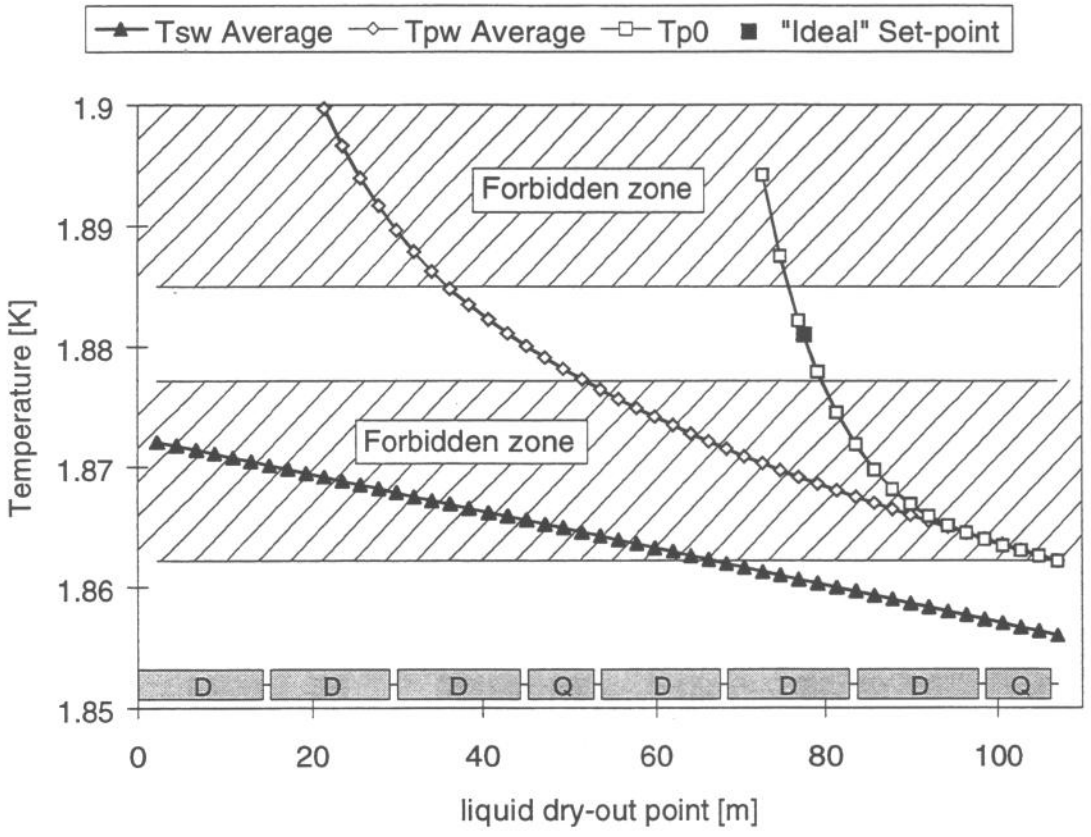

Figure 22: He II cooling loop behavior with type 4 heat exchanger

4.4. Redundancy of the He II cooling loops

In the YB version, the redundancy is based on conduction cooling by adjacent loops (if not separated by plugs). With a cooling loop of 107 m, this solution is no longer possible.

The new scheme halves the number of expansion valves TCV1. The redundancy can be implemented by adding a second valve TCV1' in parallel to valves TCV1 and subcooling heat exchangers. With such a solution, the total number of valves does not change but the following redundancies and operations can be fulfilled:

- Cooling loop redundancy in case of JT valve failure,
- Cooling loop redundancy in case of subcooling heat exchanger plugging,
- Faster cooldown of the subcooling heat exchangers

The new valves TCV1' bypass the subcooling heat exchanger and consequently, a higher vapour fraction (50 % instead of 18 %) is created during expansion through them. However, they will only be used in few cells, which renders this inefficient expansion acceptable and does not increase too much the global pumping flow. Nevertheless, the pressure drop in the cold-mass heat exchanger, and consequently the value of ΔT1, will increase. Figure 23 shows the ΔT1 increase as a function of the vapour fraction produced during the expansion. With a vapour fraction of 50 %, the ΔT1 increase is important for installed conditions but is still acceptable for nominal conditions.

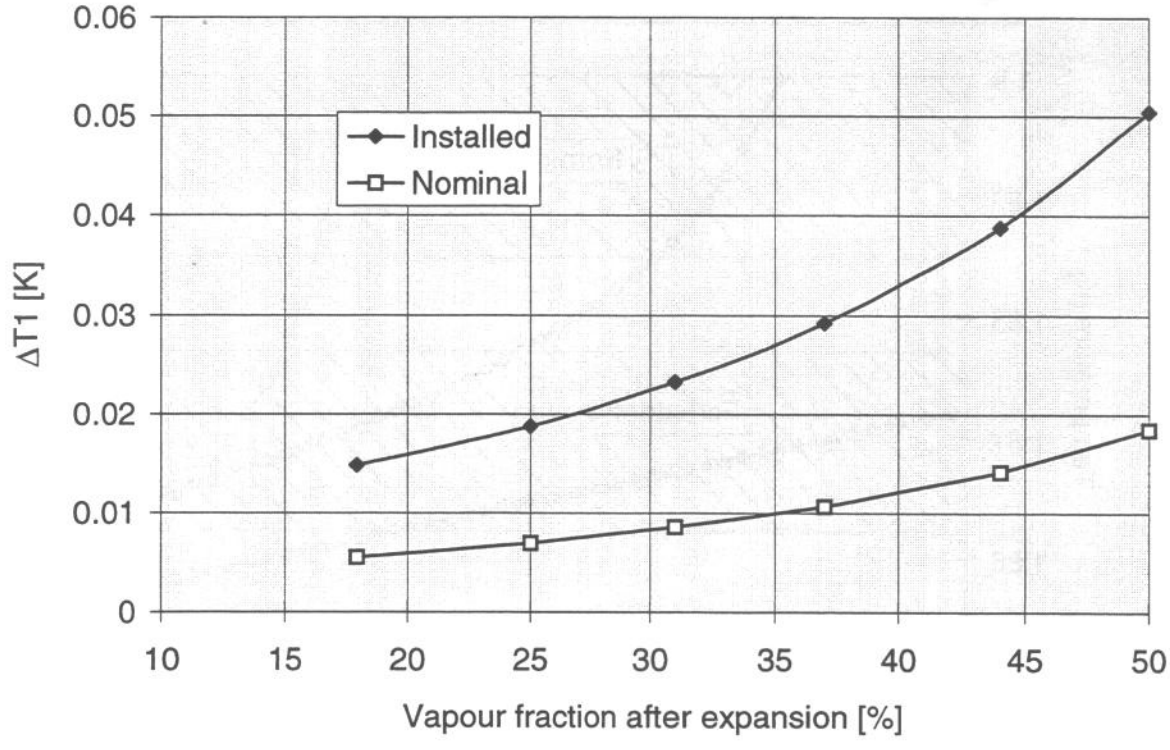

Figure 23: ΔT1 evolution versus vapour fraction after expansion

4.5. Sizing of TCV1 and TCV1′ valves

Table 9 gives the TCV1 and TCV1′ operating conditions with the corresponding flow coefficient Kv and nominal diameter DN. With respect to the YB, the flow coefficient of valves TCV1 increase but the nominal diameter stays identical (DN6).

Table 9: TCV1 and TCV1′ operating requirement and sizing

Characteristics	TCV1	TCV1′
Mass-flow [g/s]	5	24
Inlet pressure [MPa]	0.24	0.24
Inlet temperature [K]	4.9	4.9
Outlet pressure [MPa]	0.005	0.15
Kv [m3/h]	0.1	0.5
DN [mm]	6 *	6 *

* can vary depending on the valve supplier

4.6. Design of the phase separator sump

In co-current flow operation, a phase separator sump is required for detection of liquid overflow in case of control problems in the cooling loop, as well as for liquid recovery in case of liquid expulsion during a quench.

In a cylindrical tube, the amount of liquid He is smaller than in a corrugated tube. For a length of 107 m, 24 liters of liquid helium is contained in the cold-mass heat exchanger and has to be recovered in the separator pot. Inside the separator pot, a copper loop of the feed tube acting as liquid vaporizer has to be foreseen for getting rid of the liquid after an overflow.

The minimum instrumentation required is:

- A liquid helium level sensor (for liquid detection),
- A pressure sensor tapping (for saturated temperature calculation).

4.7. Recommendation and open issues

A 1.8-K cooling loop of 107 m is recommended for the simplified scheme. The corresponding cold-mass heat exchanger is constituted of a cylindrical OFHC copper tube with an internal diameter of 54 mm which fits within the existing yoke passage.

The pressure drop of the cold-mass heat exchanger could be reduced by a factor 1.5 by routing the supply pipe outside the cold mass. This solution would require a new pipe running along the cold mass in the cryostat, interconnection tightness and vacuum barrier passage, and is therefore not recommended.

5. Magnet quench and spacing of SRVs

5.1. He discharge and cold-mass pressure

During a quench, the helium contained in the cold masses is discharged through safety relief valves (SRV) which may only be installed in technical modules of the cryogenic distribution line. Decreasing the number of technical modules imposes to be able to discharge helium after a quench over a longer distance. For a length of 107 m, helium has to be discharged over a distance of 53 m if both SRV at each end open, or over a distance of 107 m if one SRV stays blocked in closed position.

Full-cell discharge has been calculated with a lumped-parameter numerical model based on energy balance and on quench discharge measurement on the Test String [6]. Table 10 gives the energies involved in the quench discharge. The energy transferred to helium is assumed to correspond to 23 % of the stored magnetic energy.

Table 10: Energies involved in a quench discharge

Quench type	Nb of open SVR [-]	Discharged Length [m]	Stored energy [MJ/SRV]	Energy transferred to He	
				[MJ/SRV]	[kJ/m]
Full String	1	40	15.3	3.5	88
Full cell	2	53	22.1	5	93
Full cell	1	107	44.2	10	93

Maximum pressure values of 12 bar have been measured on quench discharges of the full Test String with one SRV opening at 10 bar. From the point of view of length and energy, a full-cell quench with two SRVs opening at 12 bar is not far from a Test String quench with one SRV opening, and we can expect for such a quench to have a maximum pressure not far from 13.5 bar. Table 11 gives the discharge characteristics of the SRV valves.

Table 11: Discharge characteristics of SRV

Characteristics		
Flow coefficient Kv	[m3/h]	30
Opening pressure	[bar]	12
Downstream pressure (in discharge header D)	[bar]	6

Figure 24 and Figure 25 show simulation of quench discharges and give the pressure, temperature, mass-flow and valve-opening evolution during a full-cell quench with one and two SRVs opening. With two SRVs opening, the pressure increase corresponds to 12.5 bar. With only one-valve opening, the maximum pressure reaches 13.5 bar. In both cases, the maximum pressure is compatible with the design pressure of the cold-mass (20 bar).

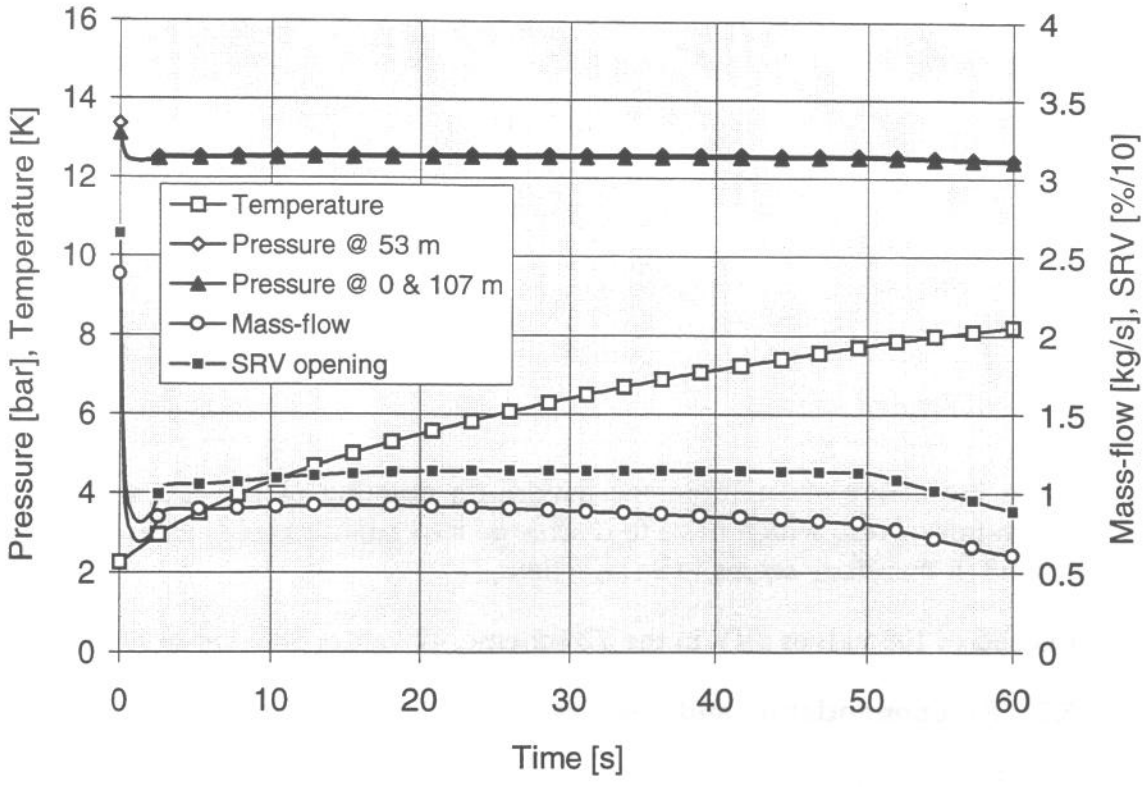

Figure 24: Simulated quench discharge with two SRV opening

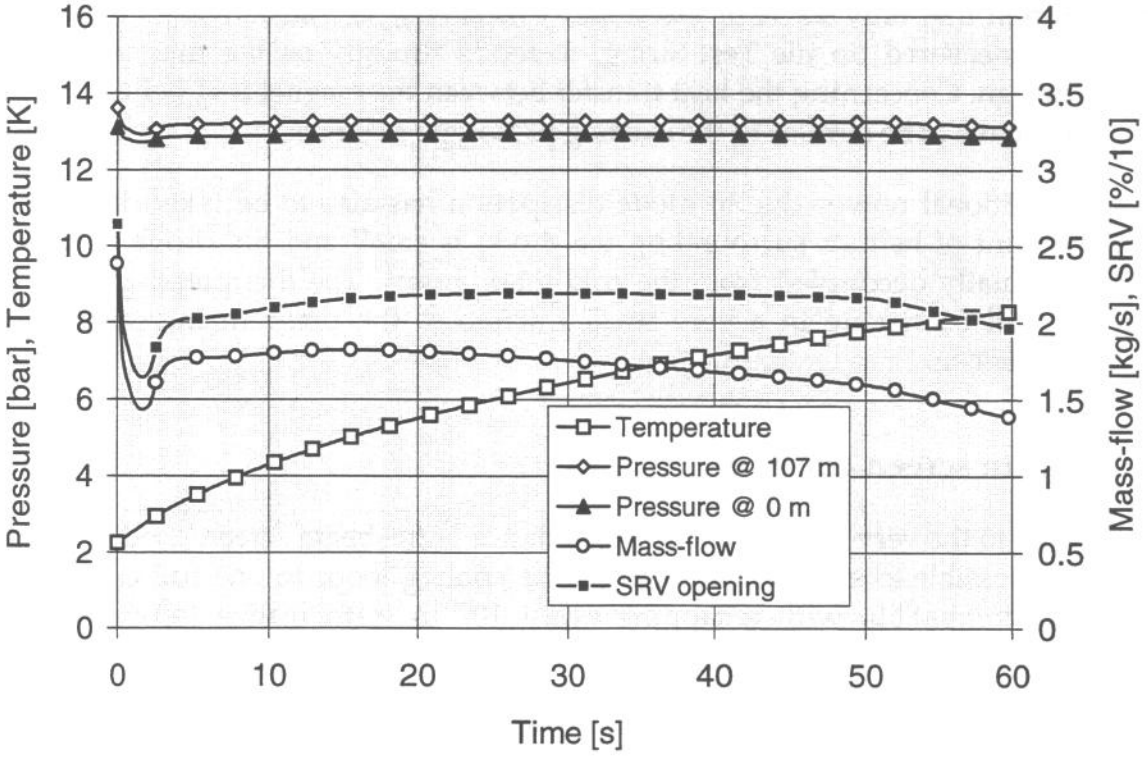

Figure 25: Simulated quench discharge with one SRV opening

5.2. SRV spacing and sizing

Safety relief valves are required every cell (107 m). In places where there are plugs, two valves are needed for discharging the two adjacent cells. Figure 26 shows the SRV valve spacing.

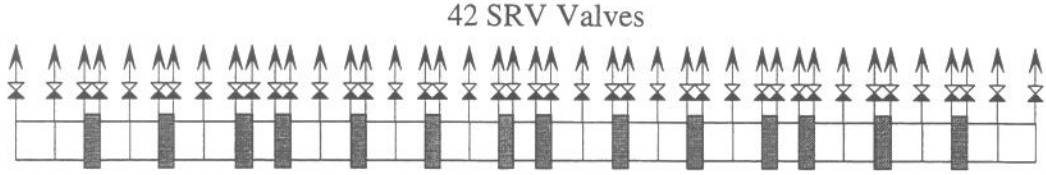

Figure 26: SRV valve spacing

From the above simulation, the maximum opening of the SRVs is less than 30 %. Even for valves, which have to discharge two adjacent cells, a flow coefficient Kv of 30 m3/h therefore seems to be sufficient.

Instead of 108 valves SRV in the YB scheme, 42 valves SRV are now required.

5.3. Recommendation and open issues

The SRV spacing shown in Figure 26 is recommended for the simplified scheme. Redundancy in case of valve blocking is preserved and a comfortable margin with respect to the design pressure is existing.

The simulation of quench discharge over a length of 107 m is based on the assumption that only 23 % of the stored coil energy is transferred to helium. This fraction, measured on the Test String, depends strongly on the magnet and cold-mass design. Concerning the heat transfer between the magnet and helium, the LHC magnets have to be similar to the existing prototype magnets.

Additional power due to diode dissipation has also to be taken into account. The amount of helium surrounding the diode is small and the diode enclosure is well thermally decoupled from the cold-mass vessel. The dissipated power in the diodes will contribute in a very small fraction to the pressure increase during a magnet quench.

6. Beam screen cooling

Due to the very high hydraulic impedance of the beam screen cooling channels, it is not possible to extend the length of the cooling loops to one full-cell. The only solution compatible with a tapping every 107 m is to realize left-right circuits. Figure 27 shows two different possibilities for such cooling loops.

From the point of control and capacity, solution 1 corresponds to the YB version. The only difference concerns the cooling of beam position monitors (BPM). In the YB version, the BPMs are thermalized around 20 K at the outlet of the beam screens. In the two proposed solutions, one BPM is cooled at the beam screen inlet, at a colder temperature (~ 7 K) which is still compatible with the BPM operation.

Solution 2, which halves the number of valves (both sides are controlled by the same valve), seems to be attractive. Such a solution could be applied only if the temperature of beam screen inlet, i.e., the heat loads before the beam screen, are identical. This condition is not fulfilled, considering the cooling asymmetry of the two sides (BPM cooling) and the possibility of having different values of insulation vacuum (different value for heat loads on 5 K screens).

Solution 1 is recommended for the simplified scheme.

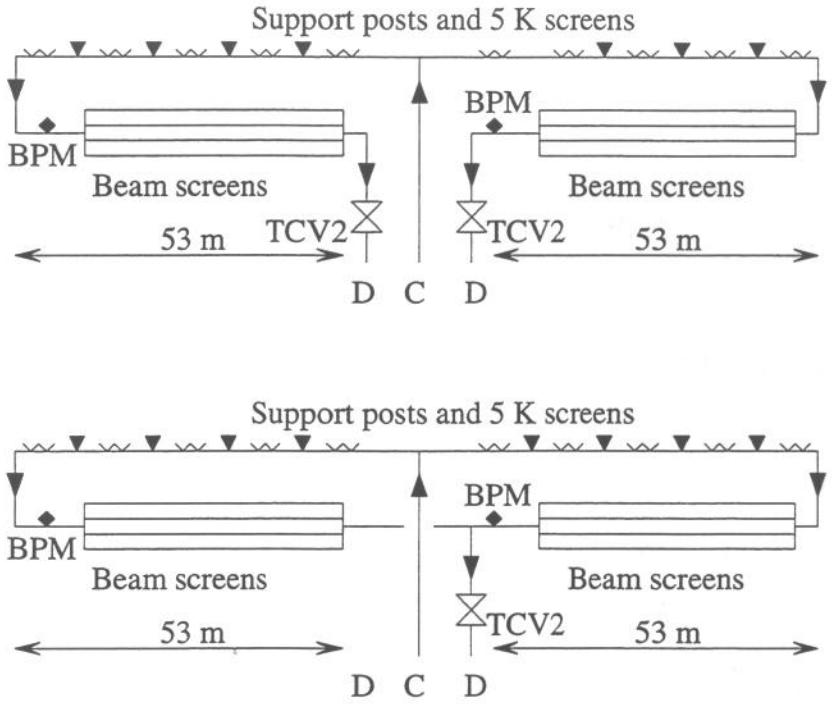

Solution 1: Left-right supply with two TCV2

Solution 2: Left-right supply with one TCV2

Figure 27: Arrangement possibilities of beam screen cooling loops

7. Vacuum barriers

In the magnet string, short intervention and magnet removal impose vacuum barriers at the location of each plug, i.e., currently every 214 m or 107 m at the sub-sector overlap.

For vacuum decoupling between the magnet string and the distribution line, vacuum barriers are also required in the jumper connection.

In the distribution line, the simplified scheme imposes no special new requirements. Vacuum barrier spacing of 428 m (equivalent to 4 full-cells) seems to be a good compromise between operating flexibility and investment cost.

Figure 28 shows the vacuum barrier spacing for an arc. Per arc, 14 vacuum barriers are required in the magnet string, 6 in the distribution line and 28 in the jumper connections. It is not possible to compare with the YB version in which the vacuum sectorization was not defined.

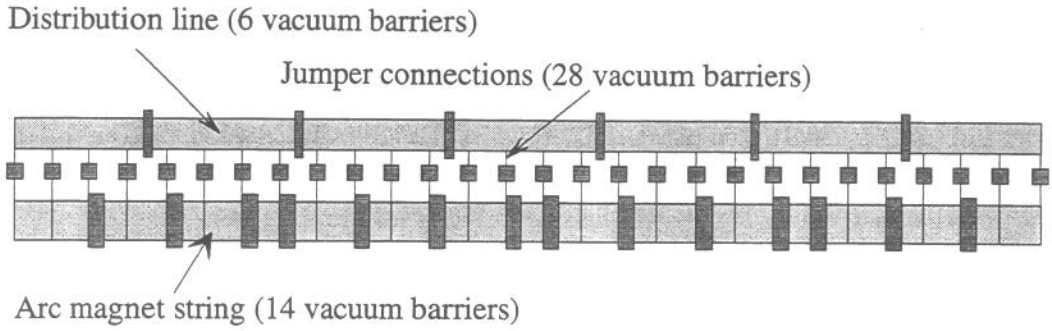

Figure 28: Vacuum barrier spacing

8. Component inventory

Inventory of different functional type of distribution line modules, jumper connections and short straight sections (SSS) can be done, putting together requirements, which concern:

- Plug spacing,
- Valve spacing (CFV, SRV, TCV1, TCV1' and TCV2),
- Sub-sector immersed valves (SSV)
- Tunnel slope,
- Need for fast cooldown valve FCV,

Table 12 gives the list of the different functional types. 6 types of distribution line modules, 4 types of jumper connections and 5 types of SSS module are listed.

The most recurrent types are:

- types 1 and 2 for the distribution line modules in which, an average of 8 valves per module (sub-sectorization valves included) have to be integrated.
- types 1 and 2 for the jumper connections in which an average of 6.5 pipes per jumper have to be integrated.
- types 0, 1 and 2 for the SSS modules. For the type 0, no cryogenic components are required.

Table 13 gives the location of the different types of modules and jumper connections. Because of the change of slope in the tunnel, a same functional type could result in mechanically different SSS modules. Table 14 gives the inventory of components required in the simplified scheme and in the YB version.

The simplified scheme saves 216 distribution line modules and 216 jumper connection. Concerning SSS modules, 216 are still existing but without cryogenic components. In particular, the simplified scheme saves 1280 valves in which 528 valves SRV are concerned.

With respect to the YB, the complexity of remaining modules and jumper connections is the same. The reduction of the number of large-diameter pipes (-0.5 per jumper) and large valves (-0.9 per module) is compensated by the increase of the number of small-diameter pipes (+1 per jumper) and small valves (+2 per module).

Table 12: Module and jumper connection functional types

Distribution line modules										
Type	Components								Location	LHC Nb
	CFV	SRV	TCV1	TCV1'	TCV2	FCV	HX	SSV		
Type 1	1	1	1	1	2	0	1	2	Arc	96
Type 2	0	2	1	1	2	0	1	2	Arc	86
Type 3	1	2	1	1	2	0	1	2	Arc	16
Type 4	1	2	1	1	2	1	1	2	Mid-arc	8
Type 5	0	2	0	0	2	0	0	2	High pt	1
Type 6	0	2	2	2	2	0	1	2	Low pt	1

Jumper connection						
Type	Interconnection pipes				Location	LHC Nb
	SRV	2 K pumping	Beam screen	2 K supply		
Type 1	1	1	3	1	Arc	96
Type 2	2	1	3	1	Arc	110
Type 3	2	0	3	0	High pt	1
Type 4	2	1	3	2	Low pt	1

Short straight section module							
Type	Components					Location	LHC Nb
	SRV tapping	2 K supply	BS supply	Vacuum barrier	Plug		
Type 0	0	0	0	0	0	Arc	216
Type 1	1	1	2	0	0	Arc	96
Type 2	2	1	2	1	1	Arc	110
Type 3	2	0	2	1	1	High pt	1
Type 4	2	2	2	1	1	Low pt	1

Table 13: Location of different module and jumper connection types

Sector	1-2, 2-3, 6-5, 8-1				4-3				4-5, 6-7				8-7			
	Slope	SSS	Jumper	CDL	Slope	SSS	Jumper	CDL	Slope	SSS	Jumper	CDL	Slope	SSS	Jumper	CDL
DS1	+	0			+	0			-	0			-	0		
		1	1	1		1	1	1		1	1	1		1	1	1
DS2	+	0			+	0			-	0			-	0		
		2	2	2		2	2	2		2	2	2		2	2	2
C1	+	0			+	0			-	0			-	0		
		1	1	1		1	1	1		1	1	1		1	1	1
C2	+	0			+	0			-	0			-	0		
		2	2	2		2	2	2		2	2	2		2	2	2
C3	+	0			+	0			-	0			-	0		
		1	1	1		1	1	1		1	1	1		1	1	1
C4	+	0			+	0			-	0			-	0		
		2	2	3		2	2	3		2	2	3		2	2	3
C5	+	0			+	0			-	0			-	0		
		2	2	2		3	3	5		2	2	2		4	4	6
C6	+	0			-	0			-	0			+	0		
		1	1	1		1	1	1		1	1	1		1	1	1
C7	+	0			-	0			-	0			+	0		
		2	2	2		2	2	2		2	2	2		2	2	2
C8	+	0			-	0			-	0			+	0		
		1	1	1		1	1	1		1	1	1		1	1	1
C9	+	0			-	0			-	0			+	0		
		2	2	2		2	2	2		2	2	2		2	2	2
C10	+	0			-	0			-	0			+	0		
		1	1	1		1	1	1		1	1	1		1	1	1
C11	+	0			-	0			-	0			+	0		
		2	2	4		2	2	4		2	2	4		2	2	4
C12	+	0			-	0			-	0			+	0		
		2	2	2		2	2	2		2	2	2		2	2	2
C13	+	0			-	0			-	0			+	0		
		1	1	1		1	1	1		1	1	1		1	1	1
C14	+	0			-	0			-	0			+	0		
		2	2	2		2	2	2		2	2	2		2	2	2
C15	+	0			-	0			-	0			+	0		
		1	1	1		1	1	1		1	1	1		1	1	1
C16	+	0			-	0			-	0			+	0		
		2	2	2		2	2	2		2	2	2		2	2	2
C17	+	0			-	0			-	0			+	0		
		1	1	1		1	1	1		1	1	1		1	1	1
C18	+	0			-	0			-	0			+	0		
		2	2	3		2	2	3		2	2	3		2	2	3
C19	+	0			-	0			-	0			+	0		
		2	2	2		2	2	2		2	2	2		2	2	2
C20	+	0			-	0			-	0			+	0		
		1	1	1		1	1	1		1	1	1		1	1	1
C21	+	0			-	0			-	0			+	0		
		2	2	2		2	2	2		2	2	2		2	2	2
C22	+	0			-	0			-	0			+	0		
		1	1	1		1	1	1		1	1	1		1	1	1
C23	+	0			-	0			-	0			+	0		
		2	2	2		2	2	2		2	2	2		2	2	2
DS3	+	0			-	0			-	0			+	0		
		1	1	1		1	1	1		1	1	1		1	1	1
DS4	+	0			-	0			-	0			+	0		

Table 14: Inventory of components

Component		Version		Variation
		SSC	YB+ Sub-sectorization	
SSS	Module number	208	424	-216
	Plugs	112	424	-312
	Vacuum barrier	112	112	0
	Separator sump	207	423	-216
Jumper	Jumper number	208	424	-216
	Large Ø pipe/jumper	2.53	3	-0.47
	Small Ø pipe/jumper	4	3	1
	Vacuum barrier	208	424	-216
CDL	Module number	208	424	-216
	4.5-2 K HX	207	423	-216
	Vac. barrier	24	48	-24
	CFV	120	432	-312
	SRV	336	864	-528
	TCV1	208	424	-216
	TVC1'	208	0	208
	TVC2	432	432	0
	Fast CD valve	8	8	0
	Sub-sector valve	416	848	-432
	Valve total	1728	3008	-1280
	Large valves/module	3.15	4.02	-0.87
	Small valves/module	5	3	2

9. Proposed basic scheme

Figure 29 shows a proposal of the simplified scheme of cryogenics for the most current types (Types 0, 1, and 2) with valves, components and interconnection piping. Figure 30 shows the singularity of the lowest point with two 1.8-K cooling circuits. This region is the most complicated arrangement of the machine, but can be integrated in the allocated volumes. This figure also shows the type 3 distribution line module with a plug, two SRV and one CFV valves.

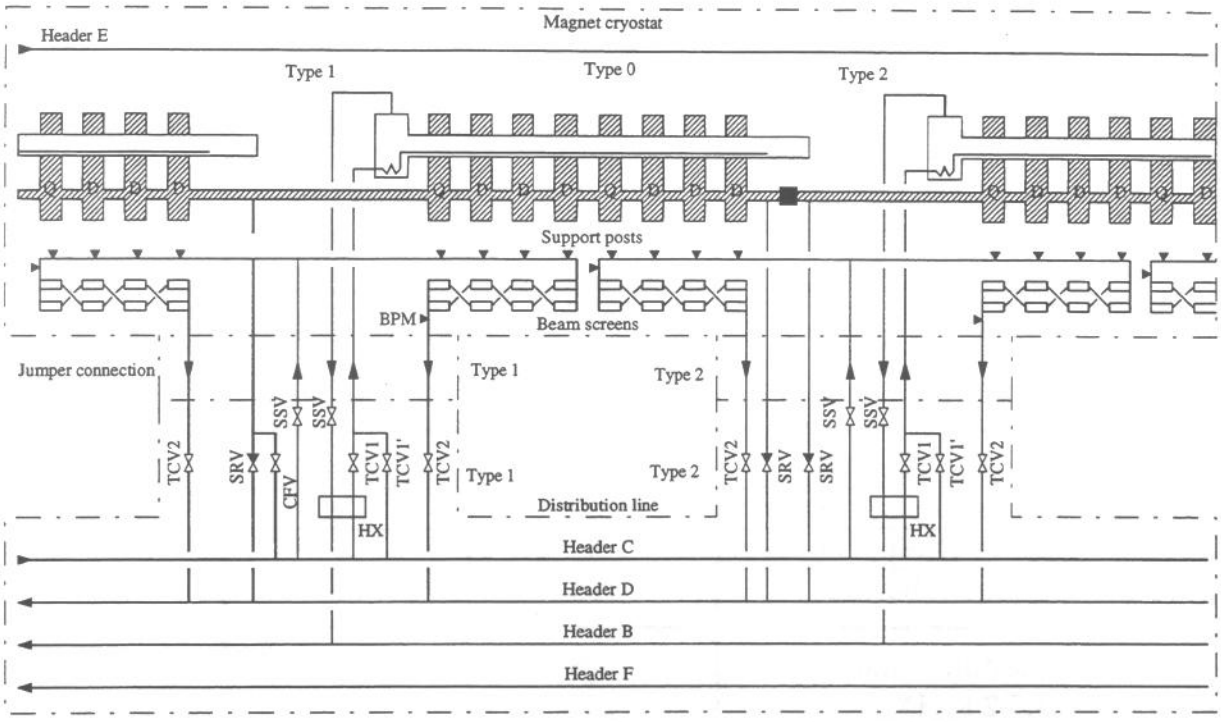

Figure 29: Basic proposal of simplified cryogenic scheme

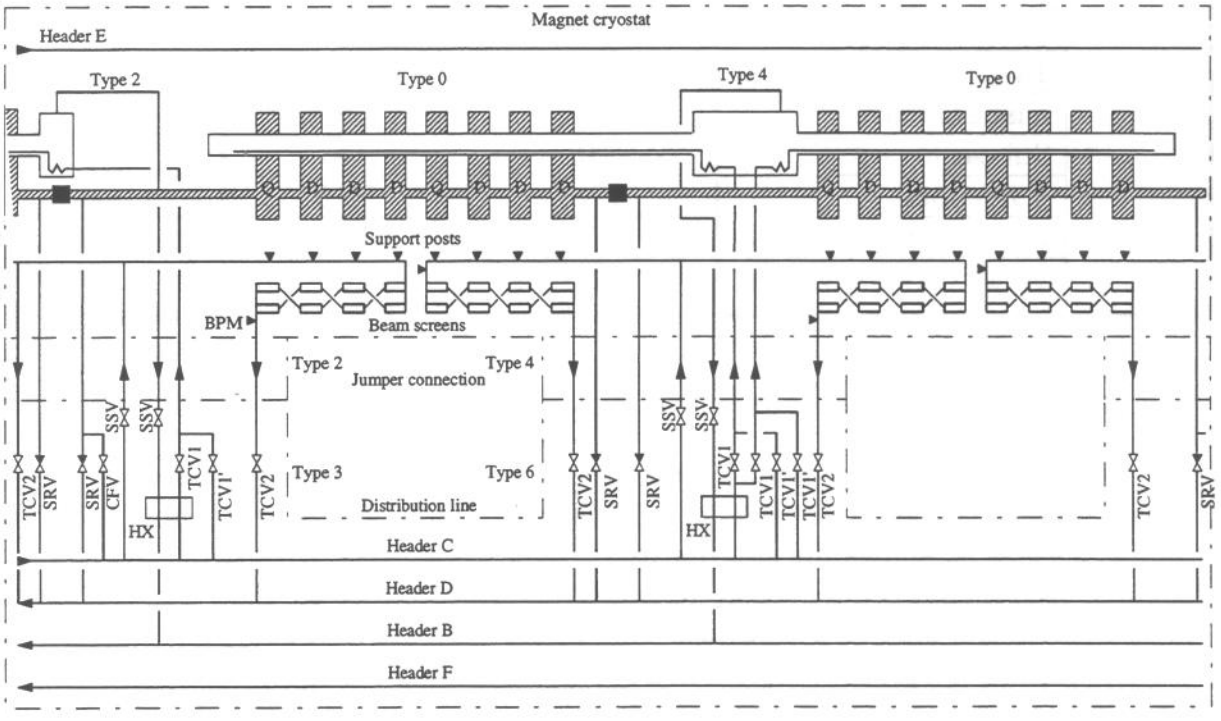

Figure 30: Low-point singularity of simplified cryogenic scheme

10. Cost savings

Table 15 gives the cost savings of the different simplifications related to half-cell and full-cell cooling.

Concerning the 1.9-K cooling loops, the simplification is globally more costly. It is due to the higher cost of the cylindrical He II heat exchanger and to the addition of TCV1' redundancy valves which increase the reliability of the cooling loops.

With half-cell cooling, the simplification concerns only reduction in number of components. A total of 7 MCHF can be saved. With full-cell periodicity, the simplification concerns both components and complete modules. A total of 26 MCHF can be saved. The simplification becomes particularly interesting when it is possible to suppress complete modules.

Table 15: Cost saving of the proposed simplified scheme

		Number		Unit price [kCHF]		Total saving [MCHF]	
		Half-cell	Full-cell	Half-cell	Full-cell	Half-cell	Full-cell
Line A suppression	Line A saving	1	1	3000	3000	-3.00	-3.00
	CCB heat exchanger saving	8	8	80	80	-0.64	-0.64
	Line A valve saving	12	12	5.6	5.6	-0.07	-0.07
	Arc heat exchanger addition	423	207	4.5	6	1.90	1.24
	Outer triplet heat exchanger additio	20	20	4.5	6	0.09	0.12
	Inner triplet heat exchanger additior	4	4	15	15	0.06	0.06
	Instrumentation addition	447	231	0.2	0.2	0.09	0.05
Sub-total line A suppression						**-1.56**	**-2.24**
Bus-bar plug and CFV spacing	plug saving	1248	1248	1	1	-1.25	-1.25
	CFV saving	312	312	4	4	-1.25	-1.25
	Process control saving	312	312	0.4	0.4	-0.12	-0.12
Sub-total bus-bar and CFV spacing						**-2.62**	**-2.62**
1.9 K cooling loop	TCV1 saving	0	216	3	3	0.00	-0.65
	Separator saving (w/o instrum.)	0	216	1	1	0.00	-0.22
	Instrumentation saving	0	216	1	1	0.00	-0.22
	Corrugated heat exchanger saving	0	1664	2	2	0.00	-3.33
	TCV1' addition	0	208	3	3	0.00	0.62
	Cylindrical heat exchanger addition	0	1664	3	3	0.00	4.99
Sub-total 1.9 K cooling loop simplification						**0.00**	**1.21**
Magnet quench	SRV saving	528	528	6	6	-3.17	-3.17
	Instrumentation saving	432	432	0.5	0.5	-0.22	-0.22
	Process control saving	528	528	0.2	0.2	-0.11	-0.11
	Sub-total magnet quench					**-3.49**	**-3.49**
Feeding periodicity	QRL module saving	0	216	81	81	0.00	-17.50
	SSS module saving	0	216	10	10	0.00	-2.16
	Sub-sector set saving	0	216	8.8	8.8	0.00	-1.90
	Straight part addition	0	216	10	10	0.00	2.16
	Instrumentation saving	0	216	1	1	0.00	-0.22
Sub-total feeding periodicity						**0.00**	**-19.61**
Total simplifications						**-7.67**	**-26.75**

11. Summary of hardware modifications

Table 16 summarizes the main modifications of the hardware with respect to the YB design and LHC Project Note 48 [7].

Table 16: Summary of main hardware modification

Hardware	Modifications
Header A	Suppressed
Vacuum barrier of distribution line	Header A passage suppressed
Subcooling heat exchanger	Nominal flow 5 g/s, distributed in cryogenic modules, maximum pressure 20 bar
CFV valves	Kv 28 m^3/h (DN32)
Cold-mass heat exchanger	OFHC cylindrical pipe with 20 % of cold work, inner Ø 54 mm, thickness 2 mm
Inner pipe of cold-mass heat exchanger	Inner Ø 10 mm, thickness 1 mm
Separator sump	Capacity of 24 liters
Jumper pumping pipe	Inner Ø 60 mm
TCV1 valves	Kv 0.1 m^3/h (DN6)
TCV1' valves	Kv 0.5 m^3/h (DN6)

12. Conclusions

The SSC working group has defined a simplified scheme of cryogenics, which fulfills the LHC requirements and preserves the (open) option of sub-sectorization. The simplifications concern:

- The suppression of header A, which is compatible with magnet temperatures below 1.9 K in nominal operation.

- The optimization of component spacing, reducing the number of passive (plugs) and active (CFVs, SRVs) components, and consequently, increasing the global reliability of the LHC operation. The proposal of SRV spacing depends strongly on the energy transferred to helium during a quench. The design of LHC series magnets, which concerns the heat transfer coefficient to helium (coil porosity, lamination density, vent passages, etc.), has to remain compatible with this spacing.

- The increase in the length of the 1.8-K cooling loops, without changing the yoke passage in the cold-mass by using a cylindrical OFHC-copper heat exchanger.

All these simplifications are compatible with a full-cell cooling In addition to component savings, the number of complete modules is significantly reduced. A total cost saving of 26 MCHF can be expected.

These simplifications increase, with respect to the YB version, the number of different types of modules. In particular, the assembly and/or tunnel installation of the distribution line and SSS have to take into account this increased complexity.

REFERENCES

[1] The LHC Study Group, "The Large Hadron Collider, Conceptual Design," CERN Report AC/95-05(LHC) (1995).

[2] A. Bézaguet et al, The LHC Test String: First Operational Experience, in: "Proceeding of EPAC96", S. Meyers, A. Pacheco, R. Pascual, Ch. Petit-Jean-Genaz and J. Poole, editors, Institute of Physics Publishing, Bristol and Philadelphia (1996), p. 358-360.

[3] Ph. Lebrun, memorandum LHC-ACR/PhL dated 6 September 1996, "Groupe de travail Simplificatiom du schéma Cryogénique du LHC".

[4] M. Bona, P. Cruikshank, W. Erdt, J.L. Périnet-Marquet, A. Poncet, P. Rohmig, U. Wagner and T. Wikberg, "Cryogenic and Vacuum Sectorization of the LHC Arcs," LHC Project Report 60 (1996)

[5] H. Guinaudeau, "Modelling counter-current two-phase flow of saturated superfluid helium in quasi-horizontal tubes: application to the LHC cryogenic system," LHC Project Note 69 (1997).

[6] B. Hilbert, "Modeling and Experimental Analysis of the Thermohydraulics of Resistive Transitions on the LHC Prototype Magnet String," LHC Project Note 86 (1997).

[7] L. Tavian, U. Wagner and R. van Weederen, "Dimensions, Fluids, Pressure and Temperature in Cryostat and Cryogenics Distribution Line Piping for the LHC," LHC Project Note 48 (1996).